

8-1-2019

The Effects of Ventilation on Trihalomethanes Removal by Spray Aeration

Alicia Qiu Cheung

Follow this and additional works at: <https://digitalscholarship.unlv.edu/thesesdissertations>



Part of the [Civil Engineering Commons](#)

Repository Citation

Qiu Cheung, Alicia, "The Effects of Ventilation on Trihalomethanes Removal by Spray Aeration" (2019). *UNLV Theses, Dissertations, Professional Papers, and Capstones*. 3745. <https://digitalscholarship.unlv.edu/thesesdissertations/3745>

This Thesis is protected by copyright and/or related rights. It has been brought to you by Digital Scholarship@UNLV with permission from the rights-holder(s). You are free to use this Thesis in any way that is permitted by the copyright and related rights legislation that applies to your use. For other uses you need to obtain permission from the rights-holder(s) directly, unless additional rights are indicated by a Creative Commons license in the record and/or on the work itself.

This Thesis has been accepted for inclusion in UNLV Theses, Dissertations, Professional Papers, and Capstones by an authorized administrator of Digital Scholarship@UNLV. For more information, please contact digitalscholarship@unlv.edu.

THE EFFECTS OF VENTILATION ON TRIHALOMETHANES
REMOVAL BY SPRAY AERATION

By

Alicia Qiu Cheung

Bachelor of Science in Civil and Environmental Engineering
University of Nevada, Las Vegas
2017

A thesis submitted in partial fulfillment
of the requirements for the

Master of Science in Engineering – Civil and Environmental Engineering

Department of Civil and Environmental Engineering
Howard R. Hughes College of Engineering
The Graduate College

University of Nevada, Las Vegas
August 2019



Thesis Approval

The Graduate College
The University of Nevada, Las Vegas

August 16, 2019

This thesis prepared by

Alicia Qiu Cheung

entitled

The Effects of Ventilation on Trihalomethanes Removal by Spray Aeration

is approved in partial fulfillment of the requirements for the degree of

Master of Science in Engineering – Civil and Environmental Engineering
Department of Civil and Environmental Engineering and Construction

Erica Marti, Ph.D.
Examination Committee Chair

Kathryn Hausbeck Korgan, Ph.D.
Graduate College Dean

Eakalak Khan, Ph.D.
Examination Committee Member

David James, Ph.D.
Examination Committee Member

Jaeyun Moon, Ph.D.
Graduate College Faculty Representative

Abstract

Chlorination has been a vital and common step employed as a primary and/or secondary disinfectant to avoid outbreaks of waterborne diseases in drinking water supplies. Besides the desired effect of inactivating pathogens, chlorine also reacts with natural organic matter and precursors in raw water to form various carcinogenic disinfection by-products (DBPs), such as trihalomethanes (THMs), four of which are (represented as total trihalomethanes or TTHM) chloroform (CHCl_3), dichlorobromomethane (CHCl_2Br), chlorodibromomethane (CHClBr_2), and bromoform (CHBr_3). Spray aeration is an effective, economical, and suitable post-treatment method commonly employed in distribution systems (e.g., storage tanks) to remove these volatile organic compounds from the water. For effective THMs removal by spray aeration in relatively enclosed systems, proper ventilation is needed to evacuate the contaminated air.

With a pilot-scale tank, this study assessed parameters associated with vent(s) and a blower to analyze their effects on the removal of the individual TTHM species. The parameters included air flow rates, blower angle, vent location, and number of vents. In addition, model simulations were conducted with the Computation Fluid Dynamics software to observe the air stream path in the headspace as the parameters changed.

TTHM removal varied under the different conditions. An average of $8.5 \pm 3.5\%$ TTHM formation occurred in the fully enclosed tank employed with spray aeration. Installing at least one vent substantially increased removals, as contaminated air was able to exit from the headspace through the openings. However, additional vents (>1) did not significant difference in removals. Locating the vent near the spray aeration nozzle (center of the tank) resulted in

slightly lower removal compared to other vent locations. Blower angle had a small effect (<5%) on TTHM removal. The differences in TTHM removal for vent location and blower angle were not statistically significant.

Increases in ventilation air flow rate proportionally increased TTHM removals, although removals of chlorinated-THMs (Cl-THMs) appeared to reach a plateau after 80 cfm air flow rate. At this flow rate, the highest overall averaged TTHM removal of 70% was attained. In addition, spray aeration alone caused a large discrepancy in the removal efficiency between the chlorinated (liquid-film controlled) and brominated (gas-film controlled) THMs. As air flow rate increased, the change in removal of brominated THMs was greater than the removal of chlorinated THMs.

These findings indicate that optimizing parameters associated with the blower and vents substantially enhances the removals of THMs in storage tanks employed with spray aeration processes. It is recommended to compare the parameters investigated in this study with other already well-known important parameters to provide water utilities with guidance on how to optimize spray aeration systems to remove THMs from drinking water supplies.

Acknowledgement

I would like to express my deepest gratitude to my advisor Dr. Erica Marti, for her continuous guidance, encouragement, and support throughout this research. This would not have been possible without your dedication to being there for me since day one.

I would sincerely like to thank several individuals. Peter Faught helped construct my experimental set-up. Tammy Jones-Lepp guided and supported through the chemical analyses with the GC-MS. Dr. Hongyang Wei and Yi-Tung Chen assisted and guided in conducting the preliminary modeling work. Dr. Dave James advised on important research calculations and topics.

Individuals at the Las Vegas Valley Water District who well deserve thanks are Mao Fang, for sparking the start of this project, and Sean Vallesteros and Steve Robertson for providing valuable information associated with my project. Thank you, Medora Corporation®, for their assistance on the research topic. I am thankful for the help from UNLV undergraduate, David Rouhani with sampling collection and analyses, and the Graduate Student Professional Association for providing financial support.

My appreciation goes to my beloved mom for her strength, support, and love. Thank you for taking good care of my younger siblings and me. Finally, I would like to express my love and gratitude for my partner, Julio, for his constant encouragement and support.

Table of Contents

Abstract	iii
Acknowledgement	v
Table of Contents	vi
List of Tables	xii
List of Figures	xiii
List of Abbreviations	xvi
Chapter 1 — Introduction, Objectives, and Hypotheses.....	1
Chapter 2 — Literature Review.....	5
■ Potable Water Supply System Processes	5
■ Chlorine.....	5
■ Chlorine Dioxide.....	6
■ Chloramines	7
■ Ozone	7
■ Ultraviolet	8
■ Hybrid Disinfection Processes.....	8
■ Potential Toxicity.....	9
■ Occurrence of TTHM in Potable Systems	10
■ Factors Influencing DBP Formation	10
■ Effects of Natural Organic Matter	11

Effect of Chlorine Dose and Bromide	12
Effects of Temperature and pH.....	12
Effect of Contact Time.....	13
Formation of Regulated DBPs Model.....	13
Detection	14
Regulations	15
Precursors Removal	16
Enhanced Coagulation	16
Granular Activated Carbon Adsorption	17
Ozone and Biological Activated Carbon	18
Advanced oxidation processes	18
Ultrafiltration/Nanofiltration.....	19
Post-Treatment.....	19
Mass Transfer.....	19
Henry's Law.....	21
The Two-Resistance Theory	22
Types of Air Stripping and Aeration Systems	23
Countercurrent Packed Towers.....	24
Diffused Aeration.....	25
Mechanical Surface Aeration.....	26

■ Spray aeration	26
■ Treatment Costs	27
■ Important Spray Aeration Parameters.....	28
■ Recycle Rates and Withdrawal Location.....	28
■ Droplet Travel Distance	28
■ Nozzle Droplet Size	29
■ Spray Cone Pattern and Angle.....	30
■ Water Temperature	30
■ Initial Bromide Concentration	31
■ TTHM species.....	31
■ Inlet Concentration of THMs.....	31
■ Free Chlorine Residual	32
■ Ventilation Air Flow Rate.....	32
Chapter 3 — Experimental Methodology.....	33
■ Pilot-Scale Tank Design	33
■ Spray Aeration Nozzle.....	34
■ Fans and Vents.....	35
■ Experimental Procedures	36
■ Sample Collection and Analytical Methods	38
■ Water Conditions	38

■ Air Conditions.....	38
■ Free Chlorine Residual	38
■ TTHM	39
■ Bulk Organic Matter (TOC).....	39
■ Bromide.....	40
■ Field and Laboratory Quality Control and Assurance (QA/QC).....	40
■ Field Duplicates	40
■ Field blanks	41
■ Calibration Blank and Quality Control Standards	41
■ Experimental Variables.....	42
Chapter 4 — Computational Methodology.....	43
■ Air Flow Modeling	43
■ Water Droplets Modeling	44
■ Application Process	44
■ Simulation Conditions	44
■ Blower angle	46
■ Vent Location.....	46
■ Results.....	47
■ Blower angle	47
■ Vent Location.....	48

■ Additional Model Simulations.....	50
■ Conclusions and Limitations.....	51
Chapter 5 — Experimental Results and Discussion	53
■ Introduction.....	53
■ Calculations and Statistics	53
■ Pilot-scale Experimental Results	54
■ Preliminary Studies.....	54
■ General TTHM Removal	55
■ Blower Angle.....	56
■ Air Flow Rates	57
■ Vent Location.....	61
■ Number of Vents.....	63
■ ANOVA Results	63
■ Water Quality and Air Conditions	64
■ Water quality.....	65
■ Air Conditions.....	67
■ Correlations.....	68
Chapter 6 — Conclusions and Recommendations.....	69
Appendix A.....	73
Appendix B.....	83

References	91
Curriculum Vitae	98

List of Tables

Table 2-1 Regulated DBPs and disinfectants under Stage 1 and 2 DBPR	16
Table 2-2 Dimensionless Henry's law constants at 25°C (Sander, 2015).	22
Table 3-1 HRT calculations based on inlet flow and volume of the tank.....	37
Table 3-2 Experimental Variables	42
Table 4-1 Parameters of the nozzle, tank, vent, and blower inlet conditions.	45
Table 5-1 Two-factor ANOVA results between air flow rates and % TTHM removals.....	61
Table 5-2 ANOVA results for the significance of each parameter on THM removal efficiency. Y represents significant ($p < 0.05$) and N represents not significant ($p > 0.05$).	64
Table 5-3 Monitored averaged water quality results for all experiments.	65
Table 5-4. Percent drop in averaged chlorine concentrations for each air flow.	66
Table 5-5 Monitored averaged air conditions for all experiments.....	67

List of Figures

Figure 2-1 Two-film resistance model. Adapted from Lewis & Whitman (1924).....	22
Figure 3-1 Pilot-scale experimental tank	34
Figure 3-2 Spray aeration nozzle: (a) side, (b) top, and (c) bottom view	35
Figure 3-3 Blower components, which include a: (a) 4-in fan with a speed controller and (b) 4-in duct with a 45° angle bend on the bottom.	36
Figure 3-4 Schematic of the pilot scale tank.....	37
Figure 4-1. Schematic of the tank for the CFD model with measurements: between the blower and tank's edge (X_1) = 6 in, tank's roof and duct tube end (X_2) = 1.5 ft, the vent and tank's edge (X_3) = 4 in, and duct bend angle (θ) = 45°. Red arrows represent the air flow directions.	45
Figure 4-2 Geometry of: Angle 1 (straight down), Angle 2 (45° from the wall), and Angle 3 (directly toward spray nozzle).	46
Figure 4-3 Geometry of: Location A) on the outer edge of the tank but near the blower, Location B) near the center of the tank, and Location C) on the outer edge of the tank.	46
Figure 4-4 Air flow streamlines path for additional simulations blower: Angle 1, Angle 2, and Angle 3. Blower only (top row) and a combination of blower and spray nozzle (bottom row).	48
Figure 4-5 Air flow streamlines path for additional simulations for vent: Location A (near the blower), Location B (near the center of the tank), and Location C (outer edge of the tank). Blower only (top row) and a combination of blower and spray nozzle (bottom row).....	49
Figure 4-6 Air flow streamlines path for air flow rates: 3 cfm, 10 cfm, 15 cfm, and 30 cfm. Blower only (top row) and a combination of blower and spray nozzle (bottom row).....	50

Figure 4-7 Air flow streamlines path for additional simulations at: Angle 1, Angle 2, and Angle 4 with 30-cfm air flow rate and vent location C. Blower only (top row) and a combination of blower and spray nozzle (bottom row). 51

Figure 5-1 Averaged formation rate of individual TTHM species in the fully enclosed pilot-scale tank. Error bars represent one standard deviation (n=4). 54

Figure 5-2 Averaged sum of formation and removal for TTHM species under different blower configurations at the same air flow rate (55 cfm) with one vent open. Formation of individual TTHM species were assumed to be equal to the averaged formation in the preliminary study of the fully enclosed tank (averaged TTHM formation $8.5 \pm 3.5\%$). 55

Figure 5-3 Averaged removal efficiencies for TTHM species for different blower configurations at the same air flow rate (55 cfm) with one vent open. Error bars represent one standard deviation (n=2-4). 57

Figure 5-4 Averaged removal efficiencies for TTHM species for different blower air flow rates with the same blower configuration (Angle 3, toward the nozzle) and with one vent open, except passive ventilation, which is with two vents open. Error bars represent one standard deviation (n=2-4). 58

Figure 5-5 Correlations between ventilation air flow rates (0-80 cfm) and individual TTHM species removal. The rates presented are 0.366 for CHCl_2Br and 0.405 for CHBr_3 60

Figure 5-6 Averaged removal efficiencies for TTHM species at different vent placements with the same blower air flow rate (55 cfm) and configuration (Angle 3, toward the nozzle). Error bars represent one standard deviation (n=2-4). 62

Figure 5-7 Averaged removal efficiencies for TTHM species with a different number of vents at the same air flow rate (55 cfm) and blower configuration (Angle 3, toward the nozzle). Error bars represent one standard deviation (n=2-4)..... 63

Figure 5-8 Correlations between inlet conditions and % TTHM removals..... 68

List of Abbreviations

Br-DBP	brominated disinfection by-product
CFM	cubic feet per minute
Cl-DBP	chlorinated disinfection by-product
DBP	disinfection by-product
DBPR	disinfection by-product rule
DOC	dissolved organic carbon
DOM	dissolved organic matter
d_{SMD}	Sauter mean diameter
DWDS	drinking water distribution system
DWTP	drinking water treatment plant
EBCT	empty bed contact time
FP	formation potential
GAC	granular activated carbon
GC-MS	gas chromatography-mass spectrometry
GPM	gallons per minute
HAA5	total haloacetic acids
HAAFP	haloacetic acids formation potential
HAAS	haloacetic acids
HANs	haloacetonitriles
HRS	hours
HRT	hydraulic retention time
LRAA	locational running annual average

LMW	low molecular weight
MCL	maximum contaminant level
MGD	million gallons per day
MRDL	maximum residual disinfectant level
NDMA	<i>N</i> -nitrosodimethylamine
NF	nanofiltration
NOM	natural organic matter
RH	relative humidity
PAC	powder activated carbon
THMFP	trihalomethanes formation potential
THMS	trihalomethanes
TOC	total organic carbon
TTHM	total trihalomethanes
UNLV	University of Nevada, Las Vegas
USEPA	United States/Environmental Protection Agency
UF	ultrafiltration
UV	ultraviolet
VOC	volatile organic compound
WHO	World Health Organization

Chapter 1 — Introduction, Objectives, and Hypotheses

Safe drinking water is fundamental for human life. However, drinking water distribution systems (DWDS) are prone to a wide range of contaminants, ranging from biological to chemical substances. To avoid outbreaks of waterborne-diseases, chlorination has been a vital and common step employed as a primary and secondary disinfectant. Besides the desired effect of inactivating pathogens, chlorine also reacts with precursor materials in raw water, mainly dissolved organic matter (DOM), forming dangerous disinfection by-products (DBPs), four of which are (represented as total trihalomethanes or TTHM): chloroform (CHCl_3), dichlorobromomethane (CHCl_2Br), chlorodibromomethane (CHClBr_2), and bromoform (CHBr_3) (Bellar et al, 1974). Due to their association with bladder and colon cancer, and premature birth (Richardson et al, 2007), the US EPA established the Stage 1 and 2 DBPR to regulate TTHM quarterly at a locational running annual average (LRAA) of $80 \mu\text{g/L}$.

Since TTHM formation is present mainly in chlorinated waters, many drinking water utilities have switched to other disinfectants such as ozone, chlorine dioxide, or chloramines. However, changing to these disinfectant agents forms new DBPs (currently up to 700) with higher toxicity (Richardson & Postigo, 2018). In addition, chlorine is still the preferred disinfectant because of its effectiveness, low cost, convenience in usage, and stability (Cotruvo & Amato, 2019; C. Li et al., 2018).

Besides altering disinfection practice, available methods to minimize TTHM formation include using treatment technologies to remove the precursor materials in raw water prior to disinfection or to target TTHM after formation within DWDS (Brooke & Collins, 2011). Granular activated carbon (GAC), enhanced coagulation, membrane filtrations, and integrated technologies

have been commonly employed to manage DBP precursors. However, these technologies may not effectively reduce the formation of DBPs to the required level in a DWDS as not all precursors (e.g., bromide) and natural organic matters—mainly DOM—are removed (Amy et al., 1991; Zainudin et al., 2018). Although membrane filtration provides the highest removal rates, it requires high capital, operation and maintenance costs.

Since a detectable disinfectant residual at the farthest location of a DWDS is required to impede pathogen regrowth (USEPA 2010), and conventional treatment processes do not remove all DOM, DBP formation is inevitable after the water exits the treatment plant. Thus, water utilities focus on TTHM removal strategies in problematic locations within DWDS (e.g., storage tanks) to prevent concentrations from exceeding the maximum contaminant level (MCL). An example technology is spray aeration, which is an effective treatment option for these volatile organic compounds (VOCs). In addition, this technology can be employed in the distribution system (e.g., storage tanks), does not need external infrastructure, and requires relatively low capital and operating costs to help meet stringent regulations in problematic areas (Brooke & Collins, 2011).

Spray aeration processes employ blowers to drive fresh air inside tanks to increase mass transfer of these VOCs between the uncontaminated air and the contaminated THM-containing water droplets. Proper ventilation prevents contaminants from saturating the headspace and re-contaminating the water.

Due to limited research on the gaseous phase of this system, this study examines the effect of design and operational parameters of the blower and vent on the removal of individual TTHM species in a relatively enclosed storage tank employed with a spray aeration system. A current issue is that existing units blow air straight down to the water surface or at an angle; however,

there is little information on why units use a particular design. In addition, in conventional tank design, a vent is installed near the center of the tank to relieve pressure from building up in the tank (AWWA, 1997). However, there is lack of research on number of vents and the vent location that would be more advantageous for TTHM removal efficiency in tanks employed with a spray aeration system. Lastly, there is a lack of information or guidance on the amount of fresh air needed to enhance the driving force for mass transfer by spray aeration.

Accounting these problems, the objectives, questions (RQ), and hypotheses addressed in this study are:

1. Investigate the effect of blower angle.

RQ: Does blower angle influence TTHM removal efficiencies? Tested blower angles are:

Angle 1) directly straight down at the water surface, Angle 2) angled 45° from the horizontal and angled 45° from perpendicular to the tank wall (i.e. not blowing directly at the tank wall), and Angle 3) angled 45° from the horizontal and toward the spray nozzle located in the center of the tank, and Angle 4) directly at the tank wall.

Hypothesis: It is expected that Angle 2 will induce the highest TTHM removal efficiency because configuring to this angle potentially creates an air flow path that follows the tank wall which should induce the best circulation in the headspace. This allows the fresh air to come into contact with most contaminants in the headspace. Angle 1 may potentially push the contaminants down back toward the water. Angle 3 may interfere with the spray pattern and cause dead spots in the tank since the path of the air does not come into contact with TTHM in certain location of the headspace.

2. Investigate the effect of the number of vents and vent location.

RQ: Does the number of vents and vent location influence the removal efficiencies of TTHM species? Tested locations are: Location A) near to the blower, Location B) near the center of the tank, and Location C) on the outer edge of the tank (farthest away from the blower).

Tested number of vents are: 1, 2, and 3.

Hypothesis: It is expected that increasing the distance between the blower with respect to the vent will increase TTHM removal. The longer distance will provide optimal circulation and prevent dead spots. The fresh air tends to travel the shortest path to leave the tank; thus, putting the vent right next to the blower will only cause the air to leave the tank with minimal contact with the TTHM in the headspace.

3. Investigate the effect of the amount of ventilation air flow rate.

RQ: Does the air flow rate discharge into the tank influence TTHM removal efficiencies?

Hypothesis: It is expected that increasing the air flow rate across the headspace will increase TTHM removal until the removal reaches a plateau. Increasing the air flow rate will cause the air to be changed more frequently over time. This is important for a relatively enclosed system to maintain a high mass transfer rate. At some point, increasing the flow rate would not change the TTHM concentration by much because maximum mass transfer is met. This will be tested by experimentally changing the blower flow rate and measuring TTHM removal in the water.

Chapter 2 — Literature Review

■ Potable Water Supply System Processes

A complete potable water supply system consists of three phases: collection, treatment, and distribution. In the collection phase, raw water is collected from either a groundwater or surface water source. Conventional treatment plants typically include a combination of coagulation, sedimentation, filtration and disinfection (World Health Organization, 2011). Water sources quality, treatment practices, and distribution systems may vary spatially and temporally among different communities depending on local conditions and circumstances (Legay et al., 2010; USEPA, 2016).

Disinfection is employed as water leaves treatment plants in order to inactivate pathogens and maintain disinfectant residuals, thereby reducing the risk of waterborne diseases. Typical disinfectants used include chlorine, chlorine dioxide, chloramines, ozone, and ultraviolet (UV) radiation. Besides UV, each has been shown to form its own set of harmful by-products, which are described below.

■ Chlorine

Historically, chlorination was pivotal in reducing the incidence of cholera, typhoid, dysentery, and other waterborne diseases during the 20th century (USEPA, 2007). Various chlorine-containing compounds are used as disinfectants, such as gaseous chlorine, calcium hypochlorite, sodium hypochlorite, and chlorine dioxide. Chlorine is a strong oxidizing and disinfecting agent. Suspended solids, inorganic/organic molecules, and microbiota in source water produce a chlorine demand, which is met when reaction with chlorine occurs. During chlorination, the relative concentrations of the hypochlorous acid (HOCl) and hypochlorite ions

(OCl⁻) are combined to be coined as “free chlorine”, which is dependent on the pH. The more effective oxidizer, HOCl, dominates at pH values <7.5 and dissociates into OCl⁻ at pH values >7.5 (USEPA, 2007). Due to its stability, it can be utilized as an effective primary and secondary disinfectant, both of which maintain free disinfectant residual in the distribution system. Chlorine is also inexpensive and convenient to use.

Despite the benefits of chlorine disinfection, there is a major issue. Rook (1974) and others discovered that an inadvertent consequence of chlorination was the formation harmful by-products (Bellar et al., 1974). Chlorine reacts with precursors, natural organic matter (NOM) such as humic and fulvic acid present in the raw water, forming various halogenated DBPs—mainly TTHM and haloacetic acids (HAAs). Five regulated haloacetic acids are chloroacetic acid, bromoacetic acid, dichloroacetic acid, dibromoacetic acid, and trichloroacetic acid. Other more recently discovered chlorinated DBP groups are haloacetonitriles (HANs) (World Health Organization, 2011). Consequently, many drinking water utilities have pursued other alternative disinfectants to meet increasingly stringent DBP regulations.

■ Chlorine Dioxide

Chlorine dioxide, a combination of chlorine and sodium chlorite, is another effective chemical biocide effective in inactivating bacteria and viruses (Padhi et al., 2018). However, chlorine dioxide may cause odor issues, can only be generated on-site, and is explosive in air at concentrations greater than 10%. Furthermore, its effectiveness reduces at low temperatures (World Health Organization, 2011).

Although chlorine dioxide does not form THMs, low THM levels may still be present due to chlorine impurities in the disinfectant (Richardson et al., 2007). Padhi et al. (2018) determined that chlorine dioxide treatment yields more HAAs than THMs (conversely, conventional

chlorination tends to produce more THMs than HAAs). Nevertheless, utilizing chlorine dioxide as a disinfectant promotes the formation of other regulated DBPs such as chlorites, chlorates (World Health Organization, 2011), and brominated DBPs (Br-DBPs) in the presence of bromide (Br^-) (USEPA, 2007).

■ Chloramines

Another chemical disinfectant, chloramines is formed by combining chlorine and ammonia. Although chloramine is less reactive than chlorine, it is persistent and maintains a biocidal efficacy; therefore, it is a prevalent secondary disinfectant (Chen et al., 2019). A disadvantage of chloramines is that they can prematurely decay, releasing free ammonia, which induces nitrification (USEPA, 2016). Therefore, the chemical equilibrium in the disinfectant breakpoint curve needs to be carefully determined in order to ensure that all free ammonia is reacted with chlorine.

Chloramination is known to produce lower levels of halogenated DBPs than chlorination (Chen et al., 2019; Padhi et al., 2018). Thus, it has been a preferred secondary disinfectant, especially at the extremities of a DWDS where DBP levels tend to be high (USEPA 2007). Unfortunately, chloramination has been associated with the formation of more toxic DBPs such as N-nitrosamines, in particular, *N*-Nitrosodimethylamine (NDMA) (Krasner et al., 2006; Marti et al., 2015; Mitch & Sedlak, 2002), iodinated THMs (Krasner et al., 2006; Richardson et al., 2007) and acids (Richardson et al., 2008), and HANs (Chen et al., 2019).

■ Ozone

Ozone, a strong oxidizing gas, is an effective chemical treatment for pathogens and trace organic contaminants. It can remove color, taste, and odor. Ozone is used on-site by introducing

air-containing oxygen over an electrical discharge through the water; it can only be used a primary disinfectant as the process does not produce a residual.

Although the use of ozone reduces the formation of THMs and HAAs, one of its main disadvantages is the formation of bromate (another regulated DBP) and Br-THMs. In high-bromide source waters, ozone oxidizes bromide (Br^-) to form the intermediate species hypobromous acid/hypobromite ion (HOBr/OBr^-), which can convert other present Br^- into bromate and/or react with NOM to form Br-THMs (e.g. CHBr_3) (Amy et al., 1991; USEPA, 2007). In addition, large doses of ozone may react with precursors to form NDMA, especially in the presence of hydroxyl radical scavengers during advanced oxidation processes (Marti et al., 2015).

■ Ultraviolet

Unlike chemical agents, UV radiation inactivates microorganisms based on photochemical reactions capable of modifying microbial DNA and RNA structures. However, it has been shown that UV may not be effective in reducing or preventing the growth of certain microbial pathogens, such as adenovirus (Gerrity et al., 2009). Similar to ozone, UV does not maintain disinfectant residuals and thus, does not protect a DWDS from bacterial regrowth. However, employing UV reduces the formation of known DBPs.

■ Hybrid Disinfection Processes

Hybrid disinfection processes are employed to reduce the formation of halogenated DBPs. For example, a combination of chlorine as a primary disinfectant, subsequently followed by chloramination as a secondary disinfectant, may be employed to reduce formation of regulated DBPs because chloramination tends to produce less halogenated DBPs than chlorine (Krasner et al., 2006). In addition, combining ozone as a primary disinfectant with chloramination or chlorine

can be effective in targeting pathogens while also reducing the formation of regulated TTHM, HAA5, and NDMA. However, ozonation followed by chlorination or chloramination shifts the speciation to the more toxic Br-THMs (Chen et al., 2019) and promotes the production of bromate and other more toxic DBPs such as halonitromethanes, and haloacetaldehydes (X. F. Li & Mitch, 2018).

Due to the complexity of disinfectant chemistry, changing disinfectant methods causes novel water issues as each disinfectant promotes new DBP classes (X. F. Li & Mitch, 2018; Richardson, 2003); new DBP classes may be more genotoxic than some regulated DBPs (Richardson et al., 2007). Currently, up to 700 DBPs have been identified (Richardson & Postigo, 2018), but a majority of those have not been as extensively researched as THMs and HAAs for their quantitative occurrence, toxicity, and available treatment technologies. Currently, water utilities employ chlorination because it is effective, economic, convenient, and provides a disinfection residual in the DWDS (C. Li et al., 2018; Liu et al., 2018). Thus, many regulations target TTHM and HAA5, the main DBP classes in chlorinated waters. Regulators also use TTHM and HAA5 as indicators for the presence of other chlorinated DBPs (World Health Organization, 2011).

■ Potential Toxicity

Based on epidemiology studies, long term exposure of DBPs through consumption of chlorinated drinking has been shown to be associated with bladder, colon, and rectal cancer (Richardson et al., 2007). A meta-analysis conducted on European males indicated that prevalence of bladder cancer increased by 47% when drinking water with concentrations of TTHM >50 ug/L compared to TTHM < 5 ug/L (X. F. Li & Mitch, 2018).

Additionally, Br-THMs (genotoxic mutagens) are known to be more carcinogenic than their chlorinated analogs (Richardson et al., 2007). Exposure to THMs via ingestion, inhalation, dermal adsorption while showering, bathing, and swimming has been shown to result in adverse reproductive outcomes and digestive cancers (Chowdhury & Champagne, 2009).

■ Occurrence of TTHM in Potable Systems

Drinking water is the main medium by which people are exposed to TTHM and HAA5. These two DBP classes are the most prevalent and largest, on a weight basis, halogenated DBPs in drinking water (Bond et al., 2012; Krasner et al., 2006; Legay et al., 2010; Richardson et al., 2007). However, TTHM and HAAs each account for ~10% of total organic halogen (TOX) (X. F. Li & Mitch, 2018). Thus, only a fraction of chlorinated organics in drinking water are identified or regulated.

Differences in TTHM and HAA5 occurrence are typically attributed to spatial and temporal variability within different drinking-water pipe distribution networks (Chen et al., 2019; Legay et al., 2010). These variations include source water characteristics, water treatment processes, system size, and DWDS specificities (Legay et al., 2010). TTHM averages in US drinking water supplies have fallen since they first began to be measured. The averages were 67 $\mu\text{g/L}$ in 1976, 42 to 45 $\mu\text{g/L}$ in 1986, and 30 $\mu\text{g/L}$ in 2013 to 2015 (Cotruvo & Amato, 2019). TTHM hotspots are typically at the furthest point from the source water and/or dead-ends where a high reaction time between the disinfectant and NOM has occurred.

■ Factors Influencing DBP Formation

The potential THM formation of a water, which is typically indicated by THM formation potential (THMFP), depends on various water quality parameters (e.g., NOM, chlorine, bromide,

pH, and temperature) and operational parameters (e.g., reaction time) (Amy et al., 1991). THMFP is equal to difference between terminal THMs and instantaneous THMs.

■ Effects of Natural Organic Matter

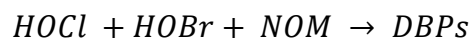
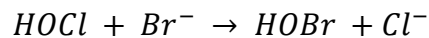
Concentration of precursors—particularly NOM—may vary spatially and temporally. For instance, ground water sources typically have a lower NOM concentration than surface water. The presence of NOM, a critical parameter of water quality, biological stability, and THMFP (Velten et al., 2011), can be quantified and characterized by surrogate parameters such as total organic content (TOC), dissolved organic carbon (DOC), UV absorbance at 254 nm (UV_{254}), and specific ultraviolet absorbance (SUVA). The last indicator, SUVA, which is equal to UV_{254} divided by DOC concentration, is commonly used as a surrogate for humic content in a water. NOM can be categorized into dissolved (DOM), which can pass through a 0.45 μm filter, and particulate organic matter (POM), which cannot. An et al. (2017) determined that after removing most DOC with molecular weight > 30 kDa, there was still a linear relationship between THMFP and low molecular weight (LMW) DOC. Thus, it can be concluded that most of THM formation is mainly attributed with the presence of DOM.

Due to the presence of carboxylic acid and phenolic groups in the NOM structure, NOM carries a negative charge drinking water conditions (Velten et al., 2011). NOM is a complex mixture of compounds which include humic substances (~50%), fulvic acids, and non-humic fractions such as proteins, amino acids, and carbohydrates (Gibert et al., 2013; C. Li et al., 2018). The THMFP of a water is primarily influenced by the concentrations and characteristics of humic substances; however, non-humic fractions can considerably account for DBP precursors as they are more difficult to analyze and remove (Bond et al., 2012; C. Li et al., 2018).

Effect of Chlorine Dose and Bromide

Higher chlorine dose generally increases formation of Cl-THMs and Cl-HAAs since more HOCl reacts with NOM. Thus, it is important to obtain a chlorine dose breakpoint at which enough chlorine residual is maintained within a distribution system, while simultaneously preventing high formation of DBPs.

The concentration of dissolved bromide present in the source waters can affect the concentration and speciation of DBPs formed (X. F. Li & Mitch, 2018; Richardson et al., 2007). In the presence of Br^- , more Br-DBPs are formed following chlorine oxidation of Br^- to hypobromous acid or hypobromite ($HOBr/OBr^-$) depending on the pH (Amy et al., 1991). Bromine induces more Br-DBPs (i.e., $CHBr_3$), whereas, HOCl produces more Cl-THMs (i.e., $CHCl_3$). Hypobromous acid/hypobromite tend to be more reactive to NOM than the hypochlorous acid and hypochlorite (Amy et al., 1991). Since chlorine is lighter than bromine, Br-DBPs can substantially increase the mass of the regulated TTHM.



Similar in concept, more iodinated THMs tend to form in the presence of iodide. Nevertheless, the presence of THM species typically follows the order: chlorinated > brominated > iodinated (Krasner et al., 2006).

Effects of Temperature and pH

For endothermic reactions, increasing temperatures is associated with the increase of reaction kinetic energy (C. Li et al., 2018). Therefore, the particle molecules are activated, promoting the reaction and therefore, increasing THMs and HAA5 formation. The DWDS are also more susceptible to microbial growth during periods of warmer water temperature; however,

it may be important to consider that a lower chlorine contact time is needed at a higher temperature to achieve the same log inactivation. (USEPA, 2007).

Similar to most chemical reactions, pH influence DBP formation; increasing it favors THMs formation, while HAAs formation is favored at a lowered pH (Bond et al., 2012; USEPA, 2010). Therefore, decreases in pH not only enhance the disinfection effectiveness, but also reduce TTHM formation. However, it is important to consider the effects of pH in the distribution system such as corrosion.

Effect of Contact Time

Contact time or reaction time is an important factor as it allows a longer time for the disinfectant and NOM to react and form DBPs (X. F. Li & Mitch, 2018). This results in water age, and typically occurs in clear wells, storage reservoirs, or pipelines. Thus, water utilities tend to enhance water flow and circulation during the design of these infrastructure such as producing tank turnovers to mitigate water quality issues and DBPs formation (AWWA, 1998). This reduces water stagnation and thus, reaction time between chlorine and precursors to form DBPs.

Formation of Regulated DBPs Model

The EPA provides a computer program, Surface Water Analytical Tool (SWAT) model, which can predict the formation of TTHM (Eq. 1 and Eq. 2) and HAA5 (Eq. 3 and Eq. 4) in raw and treated waters for systems serving >100,000 people (USEPA, 2016). Presented below are the empirical formulas included in this software.

For TTHM:

$$\text{TTHM}_{\text{raw}} = 0.0412\text{TOC}^{1.098} \text{Cl}_2^{0.152} \text{Br}_{\text{raw}}^{0.068} \text{T}^{0.609} \text{pH}_{\text{raw}}^{1.601} \text{t}^{0.263} \quad (1)$$

$$\text{TTHM}_{\text{treated}} = 23.9(\text{TOC} * \text{UV}_{254})^{0.403} \text{Cl}_2^{0.225} \text{Br}^{0.141} 1.027\text{T}^{-20} 1.156^{\text{pH}-7.5} \quad (2)$$

For HAA5:

$$\text{HAA5}_{\text{raw}} = 30\text{TOC}^{0.997} \text{Cl}_2^{0.278} \text{Br}_{\text{raw}}^{-0.138} \text{T}^{0.341} \text{pH}_{\text{raw}}^{-0.799} \text{t}^{1.69} \quad (3)$$

$$\text{HAA5}_{\text{treated}} = 41.6(\text{TOC} * \text{UV}_{254})^{0.238} \text{Cl}_2^{0.585} \text{Br}^{-0.12} 1.021\text{T}^{-20} 0.932^{\text{pH}-7.5} \quad (4)$$

where

TTHM= TTHM concentration in µg/L

HAA5= HAA5 concentration in µg/L

TOC = TOC concentration in mg/L

Cl₂ = chlorine dose in mg/L

Br = bromide concentration in µg/L

t = time in hours

UV₂₅₄ = UV absorbance at 254 nm

■ Detection

The purge and trap (P&T) gas chromatography-mass spectrophotometry (GC-MS) method is a widely known technique applied for the analysis of VOCs (e.g., THMs) in drinking water, as recommended by the USEPA (USEPA, 1996). This is also known as the dynamic headspace analysis. The P&T autosampler and concentrator system transfer a measured amount of sample

matrix into an airtight chamber. In the gas extraction, the aqueous sample is then purged with inert gas (e.g., nitrogen), which sweeps the VOCs out of the sample matrix. The volatile compounds travel into the headspace above the water and are transferred along a pressure gradient out of the chamber. The volatile compounds are then drawn along a heated line onto an analytical trap, which is a column of adsorbent material that holds the compounds by returning them to the liquid phase. A trap is a column containing multiple adsorbents. The trap is then heated, and the compounds are backflushed with nitrogen to desorb the purged sample analytes into the GC-MS column through a volatiles interface (USEPA, 1996). Compounds entering the trap will slowly elute with a measurable retention volume, which is the amount of purge gas required gas prior to elution of the analytes. THMs eluted from the GC column are identified and measured by acquiring mass spectral data for selected ions that are characteristic of individual species.

■ Regulations

Water utilities are required to simultaneously optimize the combination of disinfectants to meet pathogen inactivation goals and regulatory limits on DBPs. The US EPA requires a presence of free chlorine residual concentration of at least 0.2 mg/L to be maintained in distribution system. Additionally, since TTHM and HAAs were associated with long-term human health exposure, the US EPA established the Stage 1 DBPR for drinking water. Shown in Table 2-1, this rule enforces MCLs for TTHM, HAAs, bromate, and chlorite depending on the disinfectants employed, along with the maximum residual disinfectant level (MRDLs) (USEPA, 2010).

Stage 1 DBPR was based on a system-wide average. However, there were issues in which customers in certain locations of the water distribution system would receive elevated DBP levels although level in the whole system was below the MCLs. Subsequently, the US EPA established the most recent regulation, the Stage 2 DBPR, which builds upon the Stage 1 DBPR; however,

TTHM and HAA5 are regulated quarterly at a locational running annual average (LRAA) (USEPA, 2010). With this, each location in the distribution system needs to comply with their MCLs, and consequently, address locations prone to high DBP formation and reduce the variation of exposure for people served by different points in the distribution system (USEPA, 2016).

Table 2-1 Regulated DBPs and disinfectants under Stage 1 and 2 DBPR

DBPs	MCLs (mg/L)	Disinfectants used	MRDL (mg/L)
TTHM	0.08	Chlorine or chloramines	4.0 as Cl ₂
HAA5	0.6		
Bromate	0.1	Ozone	
Chlorite	1.0	Chlorine dioxide	0.8

TTHM—Total Trihalomethanes; HAA5—Total Haloacetic Acids; MRDL—Maximum residual disinfectant level

■ Precursors Removal

In order to manage TTHM to meet increasingly stringent regulations, water utilities employ several actions:

- Changing to other disinfectant biocides—discussed already.
- Removing precursors (e.g., NOM) in raw water during water treatment prior to disinfection.
- Targeting formed TTHM after disinfection with post-treatment technologies in the distribution system.

■ Enhanced Coagulation

Enhanced coagulation initially consists of coagulation, in which the negative charges of NOM are neutralized with positively charged coagulants. With the aid of slow mixing, the NOM and coagulants stick together to form larger flocs. This process is followed by flocculation, in which polymers are used to form connection among the flocs and gather the particles into larger agglomerates. Enhanced coagulation efficiently reduces humic acids (Gibert et al., 2013);

however, Volk et al., (2000) determined that small molecules, such as fulvic acids, are not easily removed.

Ferric chloride (FeCl_3) and aluminum sulfate or alum ($\text{Al}_2(\text{SO}_4)_3$) are common coagulants used in this process to remove THM precursors or THMFP. Gerrity et al., 2009 demonstrated that in surface water, THMFP can be reduced by 20% with 40 mg/L FeCl_3 , increasing to 50% with a pH 5.5. However, this technology can increase the relative formation of brominated-THMs (Br-THMs) because the removal of bromide \ll DOC, thereby, increasing the Br^-/DOC ratio (Amy et al., 1991; Yang et al., 2010).

■ Granular Activated Carbon Adsorption

Adsorption is a mass transfer process consisting of both physical and chemical methods of accumulating a substance at the interface between liquid and solids phases. A type of adsorption material is granulated activated carbon (GAC), which is commonly used to remove taste and odor causing compounds, DBP precursors, and other toxic compounds (USEPA, 2007). The surface of the activated carbon contains cationic functional groups, which assists in adsorbing negative net charged NOM molecules. The hydrophobicity of GAC materials prefers adsorbing DOC, especially humic substances. Moreover, low molecular weight (LMW) fractions of NOM were removed effectively because they can enter and diffuse through the pores of the absorbent (Gibert et al., 2013; Velten et al., 2011). Additionally, similar to conventional treatment—coagulation—GAC adsorption is not effective at removing inorganics (e.g., bromide), leading to the formation of Br-DBPs.

GAC has the potential to remove THM precursors, but its efficiency decreases over time due to complete saturation. Gibert et al. (2013) concluded that the efficiency of TOC removal by GAC decreased from an initial value of 65% to 40% at the end of the study. GAC adsorption is

ineffective in removing TTHM (Babi et al., 2007). However, prior research highlights the preferential adsorption of GAC for relatively hydrophobic Br-THMs as compared to Cl-THMs due to their association with higher Freundlich adsorption isotherm constants (He et al., 2018; Amy et al., 1991). Hence, GAC is a popular process to remove THM precursors as Br-THMs are less amenable to stripping via aeration (He et al. 2018).

█ Ozone and Biological Activated Carbon

The combination of ozone and biological activated carbon (O_3 /BAC) process can be effective in removing THMFP and precursors. Ozone can split the bonds in NOM and reduce their size, thereby, causing them to be more biodegradable in BAC. In a pilot-scale study, Yang et al. (2010) determined a difference of 30% in DOC removal efficiency between conventional treatment and O_3 /BAC. However, this study highlighted the increase in Br-THMFP in the presence of bromide because the Br/DOC ratio increased, and due to the fact that ozone tends to form Br-DBPs (Yang et al., 2010).

█ Advanced oxidation processes

Advanced oxidation processes are potential methods to reduce NOM and THMs. These include the combination of UV, O_3 , and hydrogen peroxide (H_2O_2). These combinations can produce hydroxyl ($\bullet OH$) radicals, which are nonspecific and capable of mineralizing DBP precursors. The percent reduction of TOC and THMFP achieved with O_3 /UV were 31% and 75%, respectively (Mohd Zainudin et al., 2018). In addition, the combination of H_2O_2 /UV could remove 80% $CHBr_3$, 99% $CHBr_2Cl$, and 75% THMFP (Mohd Zainudin et al., 2018).

■ Ultrafiltration/Nanofiltration

Membrane techniques are commonly used for desalination, but are now also being used for other purposes, including DBP control. A combination of membrane technologies, ultrafiltration and nanofiltration (UF/NF) can lower NOM and DBP formation potentials (FP) (USEPA, 2007). Yang et al. (2010) determined that UF-NF membranes can reject 88.7% DOC, 94% UV₂₅₄, 84.3% THMFP, and 97.5% HAAFP. Thus, membrane filtration is one of the best available technology for reducing THMFP and HAAFP. However, membrane filtration may not be as widely applied due to its short service life, and capital and O&M costs.

■ Post-Treatment

During the distribution phase, finished water is transported to consumers with appropriate quantity, water quality, and pressure. The removal of formed THMs after disinfection in problematic locations in the DWDS (e.g., storage tanks) may potentially reduce energy and costs required when trying to meet the regulations under the Stage 1 and 2 DBPR (Brooke & Collins, 2011; Cecchetti et al., 2014). Common post-treatment systems employed within the distribution system to physically remove THMs from the water include air stripping or aeration, which has the potential to treat a small volume of water at problematic locations. These applications are based on the principles of mass transfer and Henry's law. Thus, these systems are designed to create air and water contact to enhance mass transfer of VOCs from the liquid phase to the gas phase.

■ Mass Transfer

Mass transfer, similar to heat transfer, occurs when there is a difference of concentrations of contaminants between two regions, in this case air and water phases. This concentration gradient is responsible for the driving force, which aids contaminants to diffuse from a high concentration region to a low concentration one until equilibrium is obtained. This mass transfer

process can be described by Fick's first law of diffusion, in which the magnitude of diffusion flux (J) is proportional to the concentration gradient (dC/dy) in a volume. The one-dimensional equation of this law, assuming steady state system and absence of any convective transport, is:

$$J_A = -D_{AB} \frac{dC_A}{dy} \quad (5)$$

where J_A is the diffusion flux of component A ($\text{kg}/\text{m}^2\text{-s}$), D_{AB} is the diffusion constant of component A in a mixture of A and B (cm^2/s), and C_A is the concentration of substance A (kg/L), and y is distance of movement perpendicular to the surface of the interface (m).

Volatilization can be described as a first-order process (Roberts & Levy, 1985). The rate of mass transfer across an air to water interface ($\frac{dC_L}{dt}$) is:

$$-\frac{dC_L}{dt} = K_L a (C_L - C_L^*) \quad (6)$$

where

$$C_L^* = \frac{C_G}{H_c} \quad (7)$$

and t is time (s), K_L is the overall liquid phase mass transfer rate constant, a is the specific interfacial area (m^2/m^3), C_L is the bulk average concentration in the liquid phase (kg/m^3), and C_L^* is the liquid concentration equilibrium with the gas-phase concentration C_G (kg/m^3), and H_c is the compound's Henry's constant (dimensionless).

There is an existing liquid-gas concentration gradient to transport the mass of volatile compounds from the liquid to the gas phase. To enhance the mass transfer process by aeration, the thickness of film at air-water interface should be reduced.

Henry's Law

The principles of Henry's law are crucial when determining the environmental fate of chemicals and designing aeration systems that involve mass transfer of gases. In this gas law, with constant temperature, the amount of a given gas dissolving in a given volume of liquid (C) is directly proportional to the partial pressure of that gas in equilibrium to that liquid (P_{gas}) such that:

$$C = hP_{gas} \quad (8)$$

where h is the Henry's law constant (M/atm) and P_{gas} is the partial pressure of the gas (atm).

The suitability of a compound for removal by aeration is due to its Henry's law constant, which is widely used during mass transfer processes (Roberts & Levy, 1985). This constant can be expressed in other units or forms. To design air-stripping systems, a more commonly used form is the dimensionless Henry's law constant (H_c), which is the ratio of the concentration partitioned in air that is in equilibrium with its concentration partitioned in water. Assuming constant temperature, this constant can be determined by:

$$H_c = \frac{C_g}{C_L} \quad (9)$$

where, C_g and C_w are the gas- and liquid-phase concentrations in equilibrium, respectively.

The constituents with a larger H_c are more volatile, thereby, more strippable towards the air film (Roberts & Levy, 1985). Nicholson et al. (1984) determined the influence of temperature on Henry's law constants for THMs, which doubled approximately for each 10°C rise in temperature.

Aeration is an effective process to transfer VOCs from the water phase to air phase. THMs are VOCs because they have relatively high H_c values (Table 2-2). In addition, Cl-THMs (e.g.,

CHCl₃) are more amenable to being stripped into the air than their brominated analogs (e.g., CHBr₃). Aeration is not effective in removing HAA5 as their H_c values are low.

Table 2-2 Dimensionless Henry's law constants at 25°C (Sander, 2015).

	Species	Dimensionless Henry's law constants
TTHM	CHCl ₃	0.161
	CHCl ₂ Br	0.101
	CHClBr ₂	0.047
	CHBr ₃	0.023
HAA5	Chloroacetic acid	3.67E-07
	Bromoacetic acid	2.69E-07
	Dichloroacetic acid	3.36E-07
	Dibromoacetic acid	1.75E-07
	Trichloroethanoic acid	5.53E-07

■ The Two-Resistance Theory

Based on the Lewis-Whitman (1923) two-film model, two thin films are assumed to exist at the gas-liquid interface. The flux and equilibrium are also due to concentration gradients within these thin films (liquid and gas films), as shown in Figure 2-1.

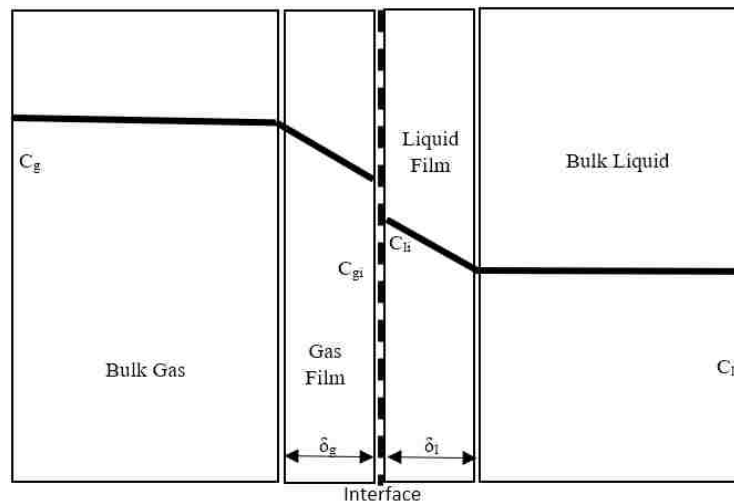


Figure 2-1 Two-film resistance model. Adapted from Lewis & Whitman (1924).

According to this theory, the total resistance, R_T , can be determined summing the individual liquid and gas phases, R_L and R_G .

$$R_T = \frac{1}{K_L a} = (R_L + R_G) \quad (10)$$

The two-film theory illustrates that highly volatile or low-solubility compounds with large H_c values are liquid-film controlled, whereas nonvolatile soluble compounds with small H_c values are gas-film controlled. Thus, Cl-THMs (e.g., CHCl_3) are more liquid-film controlled than their brominated analogs (e.g., CHBr_3), which are more gas-film controlled (Roberts & Munoz, 1985; Brooke, 2009). Thus, this model represents mass transfer as a gas phase resistance and a liquid phase resistance concept.

An advantage of this model in aeration is to determine the impact of introducing additional air volume to remove contaminants from the water to air phase. Munz & Roberts (1989) determined that K_{LA} values for volatile compounds were independent of air flow rates; however, K_{LA} values for less volatile compounds were highly influenced by air flow rates. This is due to the fact that gas and liquid resistances play a role. Thus, changing the thickness of gas film or introducing additional air are not as pronounced on removals of liquid-controlled contaminants (e.g., CHCl_3), but does influence on the rate of gas-film controlled contaminants (e.g., CHBr_3) (Brooke and Collins, 2011).

■ Types of Air Stripping and Aeration Systems

The most common forms of applying air stripping and aeration include packed towers, diffused aeration, surface aeration, and spray aeration. Aeration systems either introduce air to water (e.g., diffused aeration) or water to air (e.g., spray aeration). These systems have been developed over the years to create air and water contact enhance mass transfer of VOCs.

■ Countercurrent Packed Towers

Countercurrent packed towers are a form of air stripping that can remove fuel, ammonia, hydrogen sulfide, carbon dioxide (CO₂), and VOCs from water. In these towers, contaminated water flows down by gravity over a support packing media, while air is blown upwards from the bottom countercurrent to the water flow. The air flow strips the VOCs into the gas phase and discharges them through the top of the tower.

The performance of air stripping depends on a combination of variables. Bilello & Singley (1986) determined that THM removal efficiency was proportional to the influent air-to-water volumetric ratio and packing height, and inversely proportional to water surface loading rate. A smaller packing media provides a greater surface area, thus enhances removals. Increasing the volume of air applied at a specific water flow rate (i.e., increasing air-to-water ratio) increases removals; however, the impact of air to water ratio becomes less pronounced with greater packing depth (Bilello & Singley, 1986). Therefore, at an optimum point, it is better to increase packing height rather than the air-to-water ratio of the system. However, packing height should be limited to about 6 m (Bilello & Singley, 1986). As expected, increasing turbulence and water temperature—mainly due to effects on Henry's constant—increases removals (Roberts & Levy, 1985). In addition, removals are independent of initial concentrations, as mass transfer is only dependent on the difference between actual concentrations and equilibrium concentrations. Bilello & Singley (1986) concluded that packed-air towers obtained > 95% THMs removal.

The limitations of packed towers include the susceptibility to flooding, which is when the flow of gas interferes with the downward flow of liquid. Additionally, the need for external infrastructure and land induces high capital and O&M costs and aesthetic concerns.

Diffused Aeration

A diffused aeration system consists of diffusers, which injects air at the bottom of the tank to create bubbles. While air bubbles rise to the water surface, oxygen is transferred from the gas phase to the aqueous phase, while THMs diffuse from the water into the bubble until the point at which the bubble is saturated with the DBPs (Brooke, 2009). Once the bubbles reach the surface, they burst and introduce the THMs into the headspace.

Certain variables impact the performance of diffused aeration. The relationship of air-to-water ratio and removal rates of THMs were proportional (Bilello & Singley, 1986; Brooke & Collins, 2011). Brooke & Collins (2011) also determined that bubble size was not a vital factor on TTHM removal rates since the THMs reached saturation prior to reaching the water surface. Bilello & Singley (1986) determined diffused aeration obtain >90% THM removal efficiency in a single-stage unit; however, removals were limited using a continuous contact unit, dropping to 83%. Thus, diffused aeration was determined to be less effective than air stripping. Brooke & Collins (2011) found that CHCl_3 removals were > 90% when the air-to-water ratio was greater than 45:1. Removals were related more to the volume of air applied than to how it was applied (Bilello & Singley, 1986).

Diffused aeration is suitable and simple, as it can be employed in storage tanks or basins and relocated if needed. However, this technique is energy intensive due to the fact that the air bubbles have to be force through the large volume of water. Conventionally, water aeration has been used wastewater treatment to transfer dissolved oxygen from the air phase to water phase to support biological activities or release VOCs. Since the Henry's constant of oxygen is 100 times greater than of CHCl_3 and 1000 times than that of CHBr_3 , bubbles in diffused aeration are more prone to saturate with these DBPs; thus, a large quantity of air is required to obtain significant

transfer rates of THMs (Roberts & Levy, 1985). Therefore, diffused aeration is not suggested for water depths > 5 meters (Brooke & Collins, 2011).

■ Mechanical Surface Aeration

Mechanical surface aeration may include floating aerators that push water from under the water's surface up into the air, similarly to fountains. The water droplets then fall back into the water. Surface aeration has been conventionally used to introduce oxygen in ponds or wastewater treatments, but there is a lack of studies on this system for THMs removal.

Similar to diffused aeration, it provides the suitability of ability to be installed in reservoir tanks. However, unlike diffused aeration, surface aeration introduces the contaminants to an infinite volume of air, creating a significant larger equilibrium capacity (Roberts & Levy, 1985). This large volume of air prevents individual gases from reaching equilibrium as quickly, thereby, TTHM removal probability increases substantially.

■ Spray aeration

Spray aeration, which is the focus of this study, involves pumping water through pipelines to the nozzle, which sprays small water droplets to a large volume of air. Thus, similar to surface aeration, spray aeration exposes a small volume of contaminated water to a large volume of air, which prevents individual gases from reaching equilibrium as quickly compared to diffused aeration. Thus, TTHM removal probability increases substantially. Spray aeration is also simple and suitable because it can be employed in the DWDS (e.g., storage tanks) and relocated, unlike packed towers, which require external infrastructure. Currently, there are few studies on spray aeration for the removal of TTHM; however, costs and investigated parameters optimized for this system are presented in the upcoming sections.

■ Treatment Costs

Although these technologies can remove TOC, DOC, THMFP, and/or THMs, capital and operational and maintenance (O&M) costs must be taken into consideration. For instance, enhanced coagulation costs include chemical storage, chemical feeds, and sludge disposal (Gerrity et al., 2009). Zainudin et al., 2018 compared the annual costs associated with the different types of technologies. To treat a capacity of 3.7 million L/day, the annual costs for conventional treatments—coagulation and GAC (EBCT=15 min)—were \$1.1-\$1.3 million and \$152,000 (Zainudin et al., 2018). For AOP systems with ultrasound, the annual costs were higher, ranging from \$3.59 to \$12.5 million for 1.4 million L/day. In addition, to treat 62.5 times that capacity with UF, the annual cost was \$15.6 million. GAC seemed to require the lowest annual cost due to capability to be reactivated off-site and inexpensive cost (Zainudin et al., 2018). However, when trying to lower TTHM within a DWDS to conform to DBP regulations surface and spray aeration have the potential to substantially reduce expenses (Brooke & Collins, 2011; Cecchetti et al., 2014; Duranceau & Smith, 2016). Packed towers require only a quarter to half the operation cost of GAC with the same efficiency (Wu & Wu, 2009). Based on previous studies, diffused aeration is more energy intensive and costly than air stripping although it is more suitable and simple. Las Vegas Valley Water District (LVVWD) reported that the total one-time cost for the Gridbee® equipment and electrical work of a surface aerator was \$94,481. Similarly, spray aeration may require a capital cost <\$50,000. Overall, surface and spray aeration are suitable, inexpensive, and an effective removal processes to remove formed THMs in the distribution system.

■ Important Spray Aeration Parameters

TTHM removal by spray aeration depends on different variables, including those associated with water quality conditions (e.g., THMFP, THM speciation, and temperature) and operational parameters (e.g., recycle rates and nozzle height). It is important to consider that water quality conditions may be difficult to control in the drinking water system, whereas, the operational variables may be more practical to change. Discussion on investigated parameters in these categories and their effectiveness in optimizing the process are presented below.

■ Recycle Rates and Withdrawal Location

Based on the outputs from a sensitivity model (Cecchetti et al., 2014), the two main influential parameters were the withdrawal location of the recycle flow and amount the recycle flow. A continuous recycling from within the tank was the most efficient, accounting for >35% overall TTHM removal differences.

■ Droplet Travel Distance

Based on previous studies, nozzle height travel distance or spray nozzle height above the water surface was significant to the removal efficiency. Removal increased with an increase of nozzle height (i.e. the distance that the water droplet travels before contacting the water surface) because there is a longer contact time between the water and air (Cecchetti et al., 2014). However, the effect of increasing heights on the THM removal was less pronounced at higher heights. Cecchetti et al. (2014) observed 18.2% difference in removals between nozzle heights of 1ft and 20 ft, whereas, only 5.7% between nozzle heights of 20 ft and 45 ft. Thus, it is recommended that additional height above 20 ft does not significantly increase THM removal.

■ Nozzle Droplet Size

The nozzle droplet size, which can be changed by adjusting the pressure, is influential on TTHM removal. Based on the same model of a previous study, removal efficiency increased with decreasing the water droplet diameter, which is measured by Sauter mean diameter (d_{SMD}), with a 20% difference in reduction between small (100 μm) and large (1200 μm) droplet diameters (Cecchetti et al., 2014). The magnitude of the effect decreased with increasing water droplet diameter since the biggest difference occurred when the d_{SMD} changed from 100 μm to 300 μm .

In a pilot-scale experiment, Brooke & Collins (2011) recommended that optimizing the nozzle height is more preferable than spending energy in creating a small droplet d_{SMD} since the droplet travel distance is more influential on THMs removal. Additionally, creating a small droplet requires higher pressure, which may lead to clogging due to the buildup of hardness.

With nozzle height and diameter, Brooke & Collins (2011) focused on unit volume air to water ratio, which is the ratio of the volume of the cylinder to the volume of the water droplet. As a water droplet falls, it was assumed that the droplet travels from the exit of the nozzle as a sphere of water through a cylinder of air. The air volume is described as a long cylinder with a height (h_{avg}) equal to the average distance the droplet travels from nozzle exit to hit the water surface and a diameter equal to the d_{SMD} . The average droplet travel distance would be equal to a droplet travel path halfway between the farthest travel distance at the exterior of the spray cone and the shortest travel distance (falling vertically below the nozzle). Eq. 11 calculates the unit air to water ratio, in which h is the vertical height of the nozzle above the water surface and θ is the total spray angle.

$$\frac{a}{w} = \frac{\pi(d_{SMD}^2)h}{\frac{\pi(d_{SMD})^3}{6}} = \frac{1.5h_{avg}}{d_{SMD}} = \frac{1.5h}{d_{SMD} * \cos\left(\frac{\theta}{4}\right)} \quad (11)$$

However, this unit air to water ratio for spray aeration is not the same as ventilation air to water ratio, which was always assumed to be maximum since the headspace was presumed to be adequately ventilated to maintain the driving force, regardless of aqueous THM concentration (Cecchetti et al., 2014). Therefore, the air concentration of THMs was assumed to be close to zero; however, this is not the case in water storage tanks, which are relatively enclosed systems.

■ Spray Cone Pattern and Angle

The common type of spray cone patterns used in spray aeration systems include full-cone (uniform) and hollow-cone patterns. The uniform cone nozzle sprays droplets that are distributed uniformly in a full-cone pattern, whereas, a hollow-cone nozzle sprays concentrating on the exterior of a conical pattern. Spray angle at which the nozzle sprays was not an important parameter for uniform-cone distribution (Cecchetti et al., 2014). However, spray angle was slightly more influential for a hollow-cone pattern. Therefore, to avoid additional cost, these outputs suggested avoiding specialized spray nozzles with greater spray angles, as their effectiveness is insignificant.

■ Water Temperature

Temperature is slightly influential on TTHM removal by spray aeration. Brooke & Collins (2011) compared TTHM removal in different temperatures (i.e., 2°C, 22°C, 36°C) and determined that removals increased with increases in temperature. An average of 10% difference in TTHM reduction was concluded among the different temperatures. This is due to the fact that diffusion coefficients and Henry's constants increase with increases in temperature. However, formation of THMs also increases with higher temperatures (Nicholson et al., 1984).

Initial Bromide Concentration

As aforementioned, the concentration of precursors such as Br^- is highly influential on DBP formation and speciation. The difference in removal among the THM species by spray aeration was not significant (Brooke, 2009). Thus, the assumption was that high bromide concentration should not have an effect of the THM removals by spray aeration. However, Duranceau & Smith (2016) demonstrated that the presence of Br^- , in concentrations $> 0.10 \text{ mg/L}$, can produce HOBr , which affects the overall percent TTHM removals and THMFP of brominated species. Also, there were lower removals when more Br-THMs (e.g., CHBr_3) were present since they are less amenable to stripping.

TTHM species

Aeration generally removes more Cl-THMs (e.g., CHCl_3), as they are more amenable to stripping than the Br-THMs, which agrees with their Henry's constant. However, since THM species have dimensionless Henry's law constant of less than 0.55, mass transfer is controlled by both liquid and gas film resistance. This is important as spray aeration introduces a large amount of interfacial area of contact to the air in respect to volume of the bubble. Providing more air mixing does not have a pronounced impact on the removal of volatile species but results in greater reduction of more soluble gases that are not as efficiently treated (Brooke, 2009; Munz & Roberts, 1989). Therefore, spray aeration strips Br-THMs and TTHM much more effectively than diffused aeration.

Inlet Concentration of THMs

Removal efficiency is independent of concentration because mass transfer is only dependent on the driving force (the difference between the concentration and the equilibrium

concentration) (Bilello & Singley, 1986). It should not depend on the magnitude of the concentration in the aqueous phase.

Free Chlorine Residual

Free chlorine residual concentration is an important parameter to consider in spray aeration, as the US EPA requires a concentration of 0.2 mg/L to be maintained in the DWDS. Brooke (2009) determined that spray aeration did not influence free chlorine residual level at typical drinking water pHs. In addition, inlet free chlorine residual level was analyzed, but showed no correlation with THMs removal.

Ventilation Air Flow Rate

Spray aeration is an attractive mechanism for THM removal in the distribution system due to its potential for easy installation in existing water storage tanks, which are relatively enclosed systems. With greatly improved TTHM volatilization in these enclosed environments, proper headspace ventilation becomes a much more important consideration to remove THMs from the air volume or headspace. Stripped THMs must be removed via forced ventilation to prevent TTHM from coalescing and re-contaminating the water. Therefore, to maximize the concentration of driving force in a relatively confined space, proper ventilation with motorized fans may be required to improve removal (Brooke, 2009). There is limited research on the gaseous (air) phase of TTHM treatment by spray aeration.

Chapter 3 — Experimental Methodology

■ Pilot-Scale Tank Design

All experimental tests were conducted in a 7.5 ft (diameter) by 4 ft (height) cylindrical water storage tank (Figure 3-1); the water storage tank was designed and constructed in-house. The tank dimensions were selected because it imitates the geometry and is a scaled-down version of typical tank reservoirs in DWDS. This accommodates for the nozzle treating a 3-gpm water flow. Similarly, galvanized steel is similar to the reservoir tanks materials in DWDS as opposed to using a plastic tank.

Two corrosion-resistant, Behlen Country galvanized steel tanks were used in this study. One was flipped upside down and stacked on top of the other. The gap between the tanks was covered with HVAC foil tape to prevent air/gas from escaping the system.

The tank was located outdoors under a canopy at the University of Nevada, Las Vegas. An outdoor setting provides realistic conditions as most storage tanks in DWDS are outdoors and above ground. In addition, an outdoor setting affords a safer environment for venting TTHMs from the tank as opposed to a closed laboratory environment.



Figure 3-1 Pilot-scale experimental tank

■ Spray Aeration Nozzle

All pilot scale experiments were conducted using an “off-the-shelf” 316 Stainless Steel spray nozzle (Figure 3-2) purchased from BETE® Fog Nozzle (BETE Fog Nozzle, Inc, Greenfield, Massachusetts, 01301). The orifice diameter of the nozzle was 0.188 in. The WL-4 model sprayed at a 90° angle full cone pattern. This spray pattern was designed for low flow and medium to coarse spray atomization. A flow meter was utilized to ensure that the spray nozzle, which also functioned as the inlet, operated between 2.89 to 3.10 gallons. The pressure associated with this small range of flows was 20 psi, as suggested by the manufacturer.



Figure 3-2 Spray aeration nozzle: (a) side, (b) top, and (c) bottom view

■ Fans and Vents

A computer fan, which had a 4-in diameter, was used in the experimental tests to test low air flows as the water being treated by the spray nozzle was relatively low. For the inlet, the blower ventilated air from the atmosphere into the tank at 35, 55, 65, 75, 135, and 190 cfm. These incoming airflow rates were controlled with adjusting the speed controller of the fan (Figure 3-3a) until the vane thermo-anemometer (473B 100 mm, Dwyer Instruments Inc, Michigan City, IN, USA) measured the desired airflow rate.

A 1.5-ft duct tube with a 45° bend on the bottom (Figure 3-3b) was connected to the outlet of the blower, which was placed on the tank roof. The duct tube and bend both had a 4-in diameter; they directed the air to be discharged in the tank 1.5 ft below the tank roof at a 45° angle. This configuration was intended to enhance fresh air and water droplet contact in the tank as opposed to discharging air at the top of the tank.

There were up to three 6-in open-air vents installed to allow the air (containing THMs) to exit; they also served to relieve pressure in the tank. When the vents were not in use, they were covered with HVAC foil tape to prevent air/gas from escaping.



Figure 3-3 Blower components, which include a: (a) 4-in fan with a speed controller and (b) 4-in duct with a 45° angle bend on the bottom.

■ Experimental Procedures

Tank conditions and environmental conditions were controlled to create a consistent setting for experiments. To reduce changes in water conditions (e.g., temperature), the experiments were conducted during the evenings. Figure 3-4 presents the schematic of the tank, which was equipped with two inlet connections for the hose; one allowed the tank up to be filled with the hose directly and the second one led the water from the hose through a PVC pipe to the spray nozzle. At the beginning of the experiments, the tank was filled up to 1 ft with tap water directly with a hose. The tank was also flushed by simultaneously draining it at a lower flow. Once the water was exiting the overflow, located above the 1-ft mark, the hose was subsequently connected to the spray nozzle. To monitor the water level and activities in the tank, Plexi-glass windows were installed. In summary, tap water traveled through the hose, into the spray nozzle (acting as an inlet), and sprayed into the enclosed tank. The inflow and outflow were balanced to

ensure that the water level would remain at 1 ft. These flows were controlled by valves and monitored by a flow meter (DFC15, DIGITEN). The continuous movement and circulation of water provided mixing in the system to avoid stagnation and dead spots in the water pool.

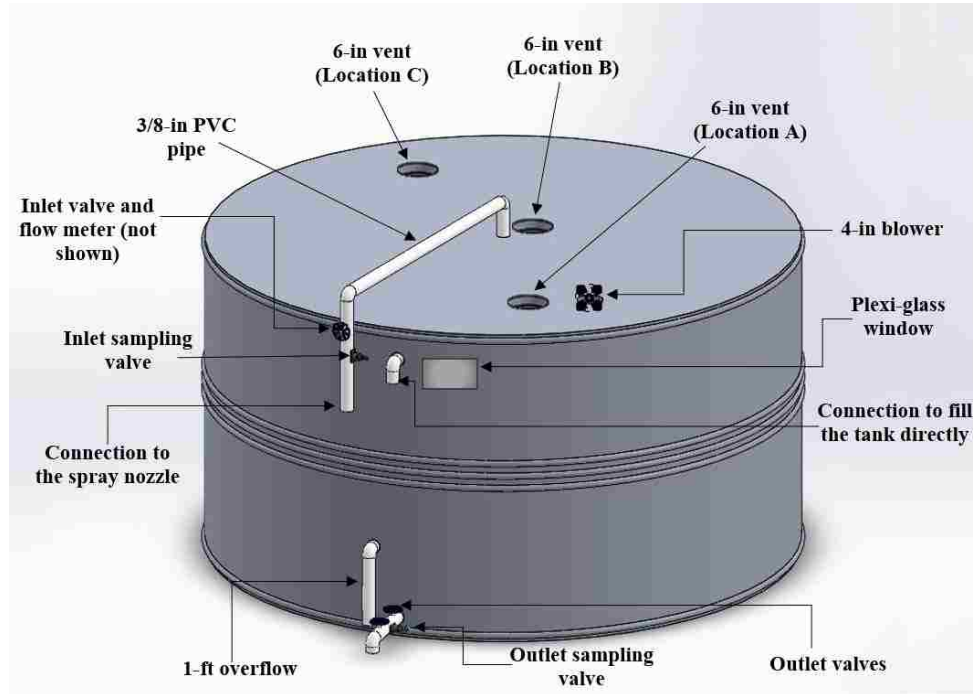


Figure 3-4 Schematic of the pilot scale tank

According to tank and operation design, the determined hydraulic retention time (HRT) was approximately 1.90 hrs (Table 3-1). Thus, inlet and outlet water samples were collected after each HRT for a total of 3 HRTs. However, only samples collected at HRT #2 and HRT #3 were used for in this study for reliability.

Table 3-1 HRT calculations based on inlet flow and volume of the tank

Tank Diameter	Water Level	Area	Volume	Q	HRT
ft	ft	ft ²	gal	gpm	hrs
7.5	1	44.2	330.5	2.90	1.90

■ Sample Collection and Analytical Methods

■ Water Conditions

The water temperature and electrical conductivity were measured on-site by a portable probe. The pH was measured by a benchtop pH meter (Orion Star A211, ThermoFischer Scientific, Waltham, MA, USA). These parameters were monitored for inlet and outlet water samples for the last two HRTs.

■ Air Conditions

The blower and vent(s) air conditions, which included air flow rate, air temperature, and relative humidity (RH) were measured by a vane thermo-anemometer (473B 100 mm, Dwyer Instruments Inc, Michigan City, IN, USA). These parameters were measured at the start of the experiment and after each HRT.

■ Free Chlorine Residual

Prior to collection, 10 mL volumetric flasks and the 10 mL spectrophotometer vials were soaked in dilute bleach to get rid of chlorine demand. This was followed by rinsing with DI water several times.

Inlet and outlet free chlorine water samples were collected with 10 mL volumetric flasks. Free chlorine residual tests were conducted right after each collection time with Method 8021: Chlorine, Free DPD Method (powder pillow) by a HACH DR/3000 spectrophotometer (HACH, USA) at 530 nm. The free chlorine residual levels were determined with a calibration curve (0.5-5.0 mg/L), which plotted the linear relationship between free chlorine residual concentration (mg/L) and absorbance. The squared correlation coefficient (R^2) for the calibration curve of 0.9913 indicated satisfactory analytical accuracy.

■ TTHM

Prior to collecting TTHM field samples, a stock solution was prepared which contained 1 g of the reducing agent, sodium thiosulfate ($\text{Na}_2\text{S}_2\text{O}_3$), in 10 mL distilled water (DI). To prevent the residual chlorine from reacting further in the water, 100 μL of the stock solution were pipetted into empty 40 mL vials. This ensured that each vial contained 10 mg of the reducing agent. Duplicate inlet and outlet TTHM samples were collected in 40 mL glass vials with Teflon septa. It was ensured that the samples did not contain air bubbles and were filled to overflowing (headspace-free). The samples were analyzed on the same day of collection or stored in a refrigerator at 4 °C.

Regulated THMs (CHCl_3 , CHCl_2Br , CHClBr_2 , CHBr_3) were detected by the GC-MS (TRACE 1300, ThermoFisher Scientific, Waltham, MA, USA) following purge and trap concentration. Reagent Restek 524.3 Trihalomethane Calibration Standard Mix was used for calibrations standards, which were included every week prior to sample analysis to ensure accuracy. Continuing calibration checks were included in every sample batch. The R^2 values for spiked samples (>0.993) indicate satisfactory analytical accuracy.

■ Bulk Organic Matter (TOC)

TOC samples were collected in 40 mL amber glass vials and acidified with 2 N hydrochloric acid (H_2SO_4) to reduce the pH to <2 based on Standard Method 5310B (acidification and sparging). This procedure converts the inorganic carbon to CO_2 . These samples were stored in a refrigerator at 4 °C in the dark until analysis. TOC concentrations were measured weekly by a TOC analyzer (TOC V-csh, Japan). The acidification generates CO_2 , which was sparged by carbon-free compressed air. The analyzer has an internal furnace, which combusts the remaining

carbon in the sample with a platinum catalyst, followed by quantification by an infrared gas detector. The R^2 values for the calibration curve >0.999 indicate satisfactory analytical accuracy.

■ Bromide

Bromide samples were collected in 60 mL glass vials and capped. Bromide levels were measured by the APHA 4500 Method: Phenol Red Colorimetric Method by a spectrophotometer (DR/3000, HACH, USA). This apparatus was set at a wavelength at 590 nm. From the 80 mL sample, 50 mL of it was added to a graduated cylinder. 2 M acetate buffer solution (2 mL), phenol red solution (2 mL), and chloramine-T solution (0.5 mL) were added. After each addition, the solution was mixed immediately. Exactly 20 min after pipetting chloramine-T, the solution was dechlorinated by adding 2 M $\text{Na}_2\text{S}_2\text{O}_3$ (0.5 mL). The bromide levels were determined from a calibration curve (0.05-0.8 mg/L) that plotted the relationship between concentrations (mg/L) against absorbance. The R^2 for the calibration curve of 0.9927 indicates satisfactory analytical accuracy.

■ Field and Laboratory Quality Control and Assurance (QA/QC)

■ Field Duplicates

Two separate inlet and outlet TTHM samples were collected after each other for HRT #2 and HRT #3. This process ensured reproducibility of the matrix and estimate sampling and laboratory analysis precision. In addition, a set of tests for each testing variable were conducted in duplicate to ensure reproducibility. Therefore, averaged values for THMs and other parameters were the average values measured in duplicate samples and experiments for two HRTs.

Field blanks

Throughout the sampling process, care must be taken to impede sample cross contamination. For each collection time, field blanks were prepared by filling the sample vial with boiled, DI water at the laboratory. The blanks taken to the sampling site, opened, and exposed to the sampling environment while the sampling is conducted, then closed and returned to the laboratory for analysis. Field blanks were used to identify errors or environmental contamination in sample collection and analysis.

Calibration Blank and Quality Control Standards

For this study, the GC-MS calibration curves and quality control standards used boiled DI water as the non-boiled DI water contained a detectable amount of chloroform and bromodichloromethane. A calibration blank containing boiled, deionized water was processed in each run by the GC-MS before sample analysis. In addition, low (1 ppb), mid (15 ppb), and high (50 ppb) QC standards were included in every TTHM analyses to check the instrument periodically for "drift"; the minimum acceptable percent of variation was 20%. Calibration standards were included every week before sample analyses to ensure accuracy.

■ Experimental Variables

Table 3-2 illustrates the variables of interest, which include blower angle, air flow rates, vent location, and number of vents.

Table 3-2 Experimental Variables

Variables	Blower Angle	Number of Vents	Air Flow (cfm)	Vent Location
Effect of blower angle at which air is being blown	Angle 1	1	55	A
	Angle 2			
	Angle 3			
	Angle 4			
Effect of air flow rates	Angle 3	2	0	A, B
		1	35	A
			55	
			65	
			80	
			135	
195				
Effect of vent location	Angle 3	1	55	A
				B
				C
Effect of number of vents	Angle 3	1	55	A
		2		A, B
		3		A, B, C

Chapter 4 — Computational Methodology

Introduction

Prior to conducting the pilot-scale experiments, a computational model was used to examine the interactions between water droplets and air flows inside the pilot-scale tank. Specifically, model simulations with Computational Fluid Dynamics (CFD) under ANSYS FLUENT 19.0 were conducted to compare different blower angles, vent locations, and air flow rates; CFD was utilized to accurately predict time-averaged water flows and air flow characteristics. The goal of this model was to use it as a preliminary source before conducting any experimental work and later to conduct a comparison of results between this model and experiments to optimize and validate the model. This aspect of the study was conducted under the guidance of Dr. Hongyang Wei.

■ Air Flow Modeling

The realizable k-epsilon (k - ϵ) turbulence model was used for the CFD simulations. The realizable k-epsilon model was picked over the standard model because the more accurate calculations for turbulent viscosity and dissipation rate were needed to capture the conditions inside the tank. The stationary wall function for high Reynolds number (Re) and no slip conditions (velocity = 0) at the wall were applied. Also, the Reynold-Averaged Navier Stokes (RANS) Equations and Boussinesq approximation were applied.

The realizable k-epsilon (k - ϵ) model solves for two transport variables: the kinetic energy (k) and the turbulent dissipation (ϵ). In this study, the governing equations were solved numerically using the CFD solver under ANSYS FLUENT. Some assumptions were constant

physical properties for air and steady state, followed by transient state (quasi-steady state) conditions.

■ Water Droplets Modeling

Conventionally, water droplet breakup can be modeled by using the Taylor analogy breakup (TAB) model, especially after exiting a spray nozzle. The governing equations in this model can determine droplet oscillation and distortion at arbitrary times. Conceptually, TAB models are based on spring-mass systems—the behavior of distorting/oscillating droplets is captured by modeling surface tension after the restoring force of a spring and the external force after the aerodynamic force (O'Rourke & Amsden, 2010). Additionally, TAB models can account for the relative motion between droplets and gas, as well as the effects of liquid viscosity of small droplets.

■ Application Process

Initially, the generation of geometry in the system, such as the shapes and sizes of the tank, nozzle, and blower; geometries was created with ANSYS DesignModeler. This is followed by the creation of the mesh in ANSYS Meshing by generating a grid with small-sized cells.

■ Simulation Conditions

Parameters associated with the tank, spray nozzle, and blower were included in the model simulation. The schematic of the tank Figure 4-1 depicts distances: between the blower and tank's edge (X_1), between the tank's roof and duct tube end (X_2), and between the vent and tank's edge (X_3). The duct bend angle (θ) was 45° . The red arrows represent the direction of air flow. In this model, initial conditions began at the exit of the spray nozzle, so that any water droplets behavior prior to exiting the nozzle was neglected. In addition, since the water level remained constant and

the focus was in the headspace, the water pool was neglected. Lastly, water droplets were assumed to drop to the pool once contact was made with the walls of the tank.

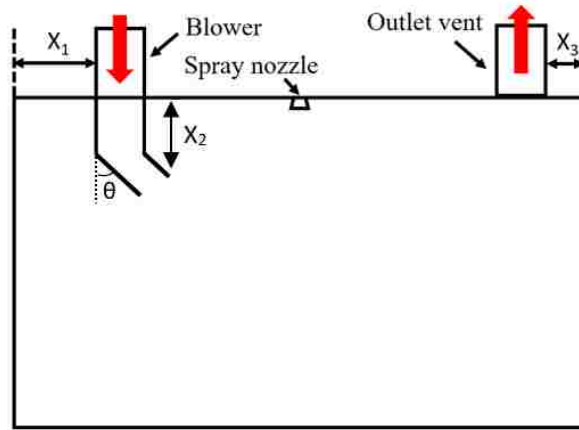


Figure 4-1. Schematic of the tank for the CFD model with measurements: between the blower and tank's edge (X_1) = 6 in, tank's roof and duct tube end (X_2) = 1.5 ft, the vent and tank's edge (X_3) = 4 in, and duct bend angle (θ) = 45° . Red arrows represent the air flow directions.

Additional crucial model inputs are described in Table 4-1 below.

Table 4-1 Parameters of the nozzle, tank, vent, and blower inlet conditions.

Nozzle					Tank				Blower Inlet		Vent
Orifice $d^{(1)}$ (in)	Spray Angle (deg)	$Q^{(2)}$ (gpm)	Pressure (psi)	$d_{SMD}^{(3)}$ (μm)	$d^{(1)}$ (ft)	Height (ft)	Water Level (ft)	Air Height ⁽⁴⁾ (ft)	$Q^{(5)}$ (cfm)	$d^{(1)}$ (in)	$d^{(1)}$ (in)
0.188	90	2.89	20	420	7.5	4	1	3	10	4	6

⁽¹⁾ diameter; ⁽²⁾ inflow rates, which equals the outflow exiting the tank; ⁽³⁾ Sauter mean diameter provided by the manufacturer specifications for the nozzle; ⁽⁴⁾ headspace; ⁽⁵⁾ blower air flow rate

Simulation cases were conducted to compare the different flow conditions produced by various boundary conditions. A critical parameter in this study was air flow rate. Thus, different scenarios were modeled for air flow rates at 10, 15, and 30 cfm. Additional parameters are pictured below (Figure 4-2 and Figure 4-3):

Blower angle

Figure 4-2 presents the three of the blower angles investigated in this study, using parameters in Table 4-1 and vent Location A.

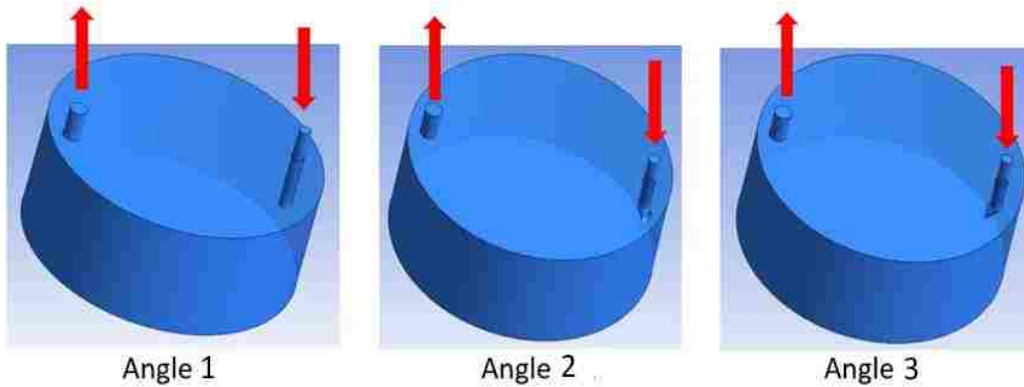


Figure 4-2 Geometry of: Angle 1 (straight down), Angle 2 (45° from the wall), and Angle 3 (directly toward spray nozzle).

Vent Location

Figure 4-3 presents the vent locations investigated in this study, using parameters in Table 4-1 and Angle 2.

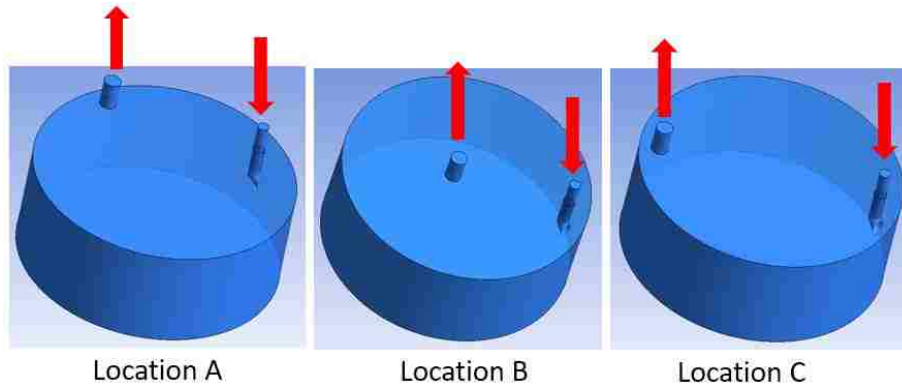


Figure 4-3 Geometry of: Location A) on the outer edge of the tank but near the blower, Location B) near the center of the tank, and Location C) on the outer edge of the tank.

■ Results

■ Blower angle

The blower angle and presence of the spray nozzle both produced large differences in the air streamline within the headspace. Figure 4-4 presents the modeling results for the blower angles at which 10-cfm air flow rate was being discharged. The top row represents air streamline conditions when employing a blower only (no spray nozzle). The bottom row represents the air streamline conditions for employing a combination of a blower and a spray nozzle. For Angle 1 (top row) without the presence of the nozzle, the streamline was slow and short; the air seemed to be stagnant in the tank. However, this was different with the presence of the nozzle (bottom row); in this case, the water droplets induced more air movement because the velocity of droplets exiting the spray nozzle was substantially greater than that of the air.

The model indicated that Angle 2, at which the blower discharged air at a 45° angle away from the wall, produced beneficial results for cases in both the top and bottom row. With this angle, employing a combination of the blower and nozzle generated homogeneous air circulation around the tank, thereby preventing TTHM from coalescing in dead spots. Of the angles with the nozzle operating (bottom row), Angle 3 performed the worst because it produced a large dead spot in the headspace due to slow air movement on one side of the tank. This was due to high velocity droplets pushing slower gas molecules toward the outer edge of the tank, where the vent was located.

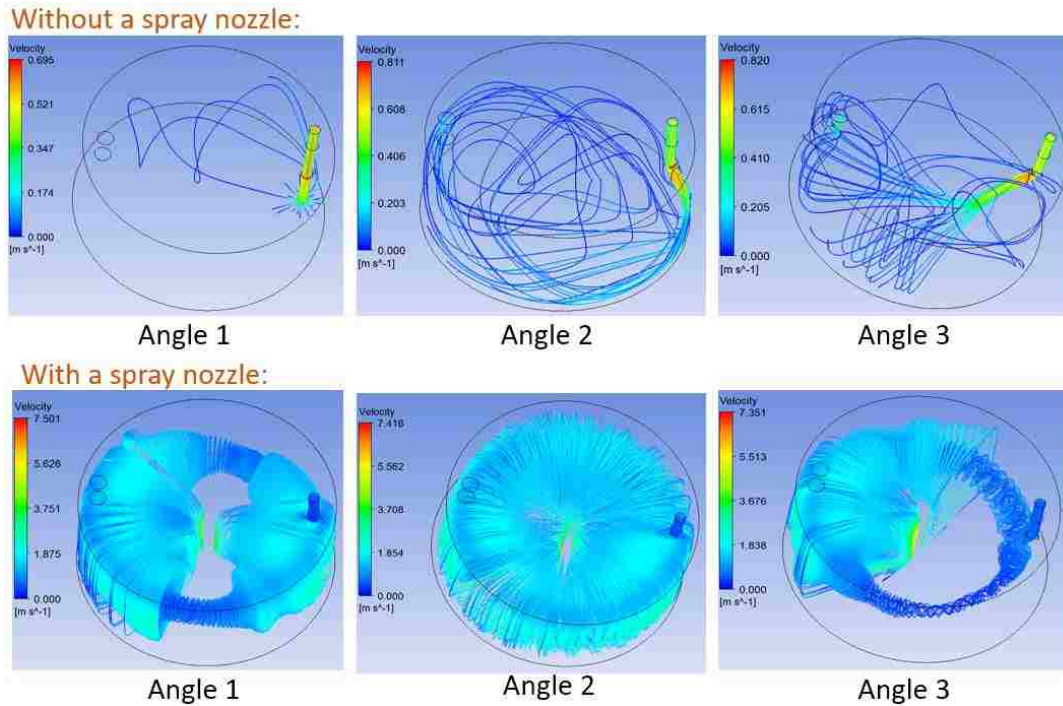


Figure 4-4 Air flow streamlines path for additional simulations blower: Angle 1, Angle 2, and Angle 3. Blower only (top row) and a combination of blower and spray nozzle (bottom row).

■ Vent Location

Vent location appear to have a slight influence on the streamline of fresh air in the headspace. Figure 4-5 illustrates that the movement of fresh air in the headspace were similar for Locations A and C. In these cases, the air streamline was homogeneous within the headspace. The streamline of fresh air in Location B performed the worst because it did not effectively target all locations in the headspace, thereby, producing dead spots. Dead spots are disadvantageous because they may potentially allow THMs to coalesce. In addition, there is large dead spot in the center of the tank, indicating that water droplets may potentially act as an obstruction to the airflow from exiting the tank if the vent is located near the center.

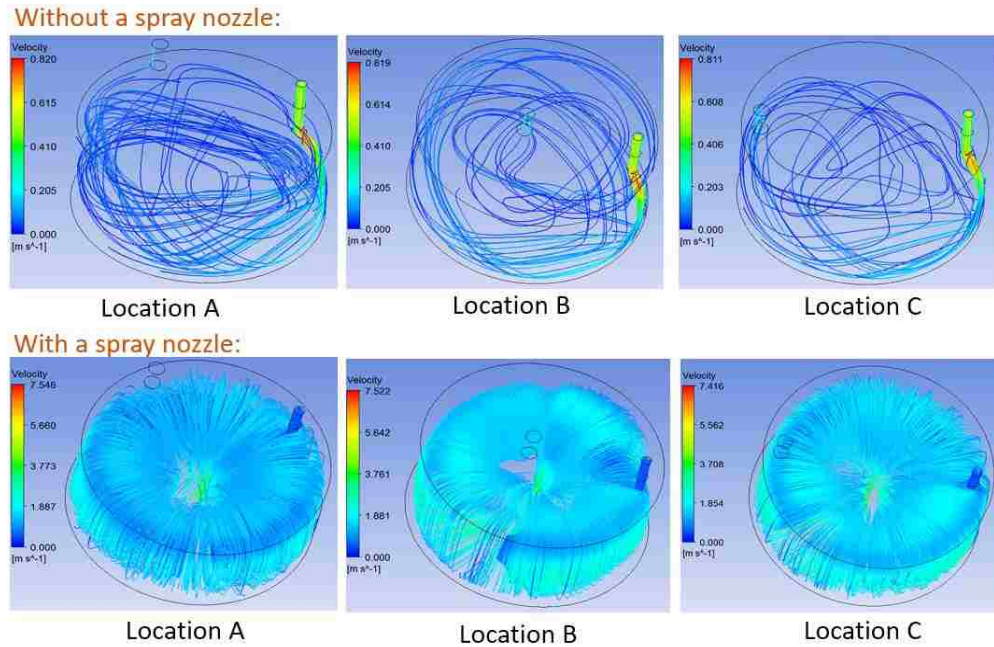
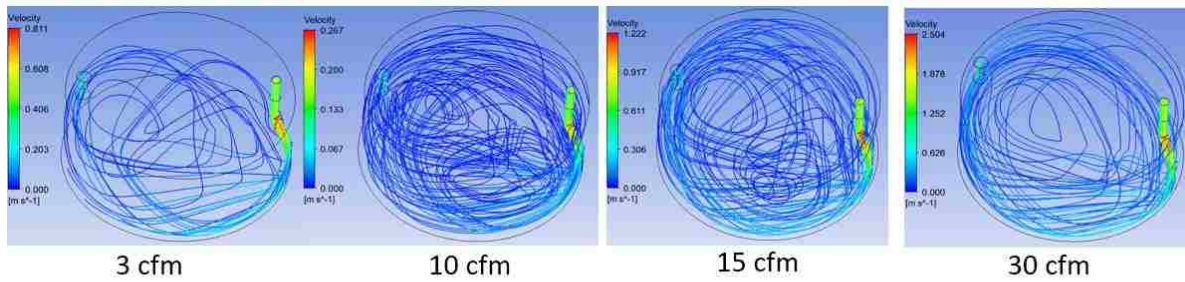


Figure 4-5 Air flow streamlines path for additional simulations for vent: Location A (near the blower), Location B (near the center of the tank), and Location C (outer edge of the tank). Blower only (top row) and a combination of blower and spray nozzle (bottom row).

Air flow rates appeared to have an influence in the gaseous streamline path. Figure 4-6 presents the model results for 3 cfm, 10 cfm, 15 cfm, and 30 cfm. As expected, increases in inlet air flow rates produce better mixture behavior. The lower air flow rates—3 cfm and 10 cfm—formed more dead spots in the headspace. However, air flow rates of 15 cfm and 30 cfm difference more homogeneity in the gaseous streamline. Thus, experimental work is required to test these air flow rates to determine actual TTHM removal efficiencies in the water.

Without a spray nozzle:



With a spray nozzle:

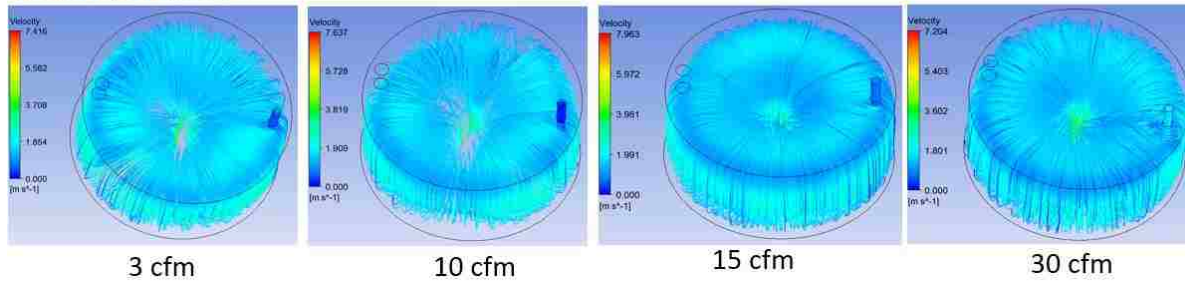


Figure 4-6 Air flow streamlines path for air flow rates: 3 cfm, 10 cfm, 15 cfm, and 30 cfm. Blower only (top row) and a combination of blower and spray nozzle (bottom row).

Additional Model Simulations

Once the individual parameters were optimized in this sensitivity-analysis, the same blower angles were simulated again, but this time with an inlet air flow rate of 30 cfm. However, Angle 4, which represents an angle at which the air is discharged directly at the wall, was used instead of Angle 1. Figure 4-7 presents the modeling results of these cases.

Angle 2 again produced the best air flow streamline path. In addition, discharging air at the wall directly for Angle 4 reduced homogeneity of the air flow behavior when compared to Angle 2. The reason for this was that the energy of the air molecules would be reduced substantially after impacting with the wall, thereby, reducing efficiency of the blower.

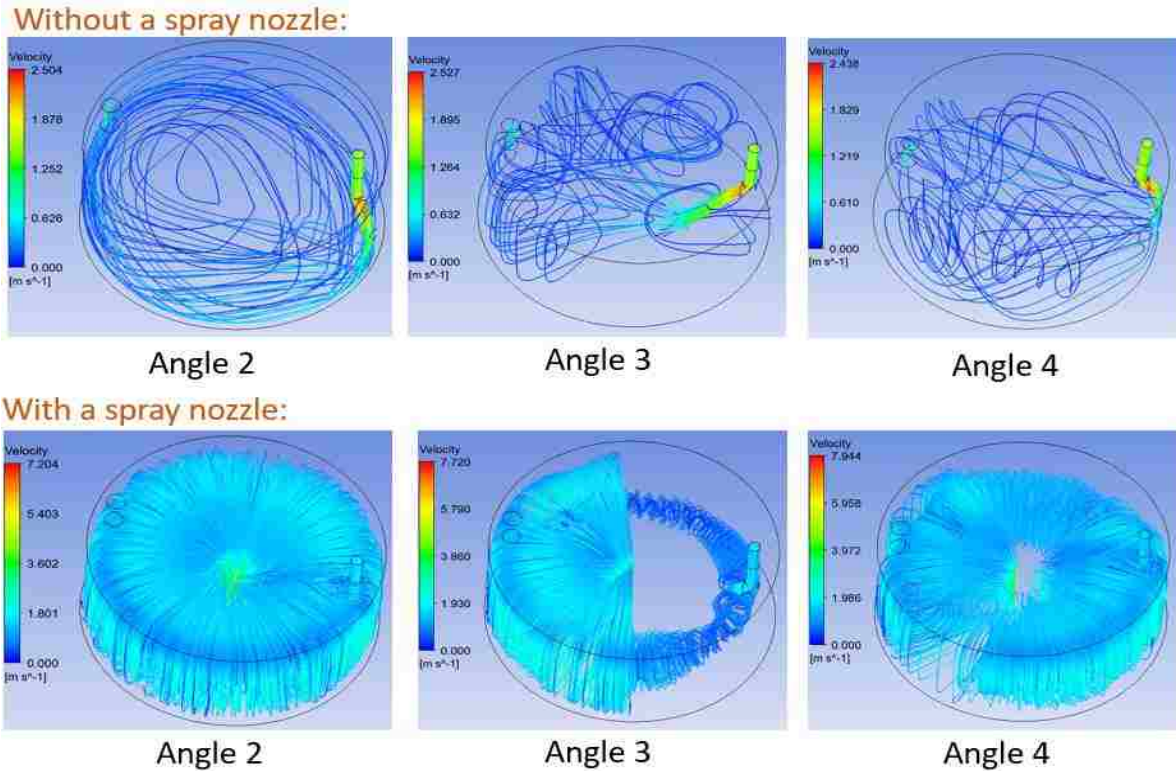


Figure 4-7 Air flow streamlines path for additional simulations at: Angle 1, Angle 2, and Angle 4 with 30-cfm air flow rate and vent location C. Blower only (top row) and a combination of blower and spray nozzle (bottom row).

■ Conclusions and Limitations

From this modeling work, it can be concluded that the blower configuration, vent location, and air flow rates produce different air streamline paths, which is an important indicator of the water droplet and air interactions and, thus, TTHM removal. Water droplets influence air flow behavior, since droplet velocities are much greater than air velocities; the reverse is not true. It can be concluded that air flow behavior is influenced by water spray from the nozzle. Finally, the model indicated that blowing 30 cfm at a 45° angle from the wall, along with placing the vent as far as possible from the blower produced the best airstream line path in the headspace.

Besides the limitations and restrictions included in the model, a limitation in these simulations was neglecting chemical interactions of TTHM, water, and air due to time constraints.

However, the goal of this model was to provide preliminary information before conducting any experimental work. The next step was to conduct the pilot-scale experiments to compare with the results obtained by the model.

Chapter 5 — Experimental Results and Discussion

■ Introduction

Spray aeration processes are effective, suitable, and inexpensive to remove THMs, which are volatile compounds, in drinking water supplies. In this pilot-scale experiment, ventilation parameters (i.e., angle blower, air flow rate, vent location, and number of vents) were investigated to optimize spray aeration processes by measuring the concentrations of individual TTHM species concentration of the inlet (untreated) and outlet (treated) water. Water quality and air conditions were monitored throughout the experiments to ensure stability. In addition, conclusions from this data were also compared to results from the model described in Chapter 4.

■ Calculations and Statistics

THM removal was calculated as the percentage change between the inlet and outlet concentrations. Technically, this percentage change is a combination of THM removal through volatilization via spray aeration and THM formation during the one HRT before sample collection. For simplicity, these combined processes are jointly considered as THM removal.

Removal was calculated for each of the four THM species, as well as TTHM. Since the THM species have different masses, the concentrations were adjusted as follows before summing the inlet and outlet concentrations (Abdel-Wahab et al., 2010):

$$TTHM = CHCl_3 + 0.728 * CHCl_2Br + 0.574 * CHClBr_2 + 0.472 * CHBr_3 \quad (12)$$

Statistical analyses for Student's t-test (t-test) with paired-samples were conducted for each water quality parameter to identify the statistical significance between inlet and outlet water samples with a 95% confidence level ($p < 0.05$). In addition, monitored air conditions were also analyzed for statistical significance between the blower and vent. All water quality, air condition

parameters, and inlet TTHM concentrations were evaluated for potential correlations with % THM removals. One-factor analysis of variance (ANOVA) tests were conducted to determine the significance of each tested parameter on % TTHM removal with 95% confidence level.

■ Pilot-scale Experimental Results

■ Preliminary Studies

Before the vents and the blower were installed, tests were conducted with the spray aerator employed in the fully enclosed tank. No removals occurred, but in fact THMs formed in the tank, although the water was being treated with spray aeration (Figure 5-1). The overall averaged adjusted TTHM formation was $8.5 \pm 3.5\%$. The free chlorine residuals continued to react with precursors in the water pool. This is illustrated with the $16.5 \pm 5.3\%$ decrease in chlorine concentrations between the inlet and outlet samples. In addition, the formation percentage of CHCl_3 was the highest among the species, followed by CHCl_2Br , CHClBr_2 , and CHBr_3 , respectively. This is expected, as presence of TTHM speciation in tap water is typically in the following order: $\text{CHCl}_3 > \text{CHCl}_2\text{Br} \approx \text{CHClBr}_2 > \text{CHBr}_3$ (Legay et al., 2010).

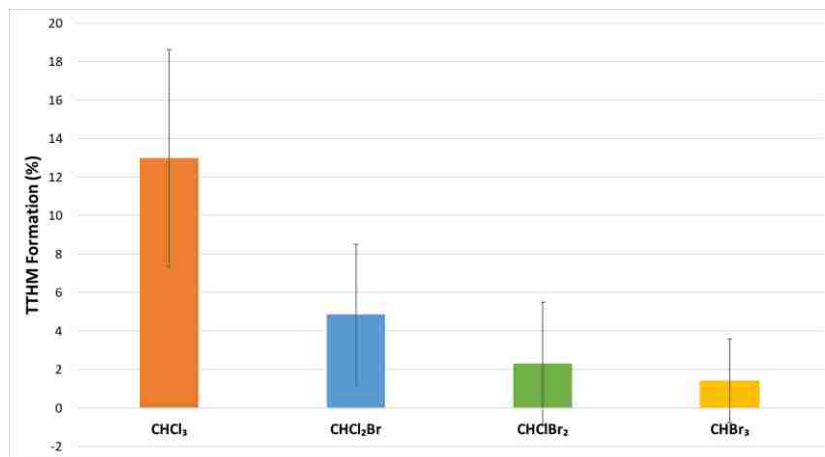


Figure 5-1 Averaged formation rate of individual TTHM species in the fully enclosed pilot-scale tank. Error bars represent one standard deviation (n=4).

General TTHM Removal

Across all experiments, change in CHCl_2Br concentration between the inlet and outlet was the highest. This was unexpected, since CHCl_3 has been found to be the most amenable to stripping in previous studies (Brooke & Collins, 2011; Clark, 2016; Duranceau & Smith, 2016). As aforementioned in Section 5.3.1, this may have been due to the relatively higher CHCl_3 formation in the tank compared to CHCl_2Br . Thus, if formation in the water tank is assumed equal to the average formation in the preliminary studies, the actual CHCl_3 removal efficiency may be closer to those of CHCl_2Br (Figure 5-2). The removal of CHBr_3 was the lowest, as expected based on its low Henry's Law constant. Previous studies concluded that THM speciation had minimal effects on removal efficiency by spray aeration compared to diffused aeration (Brooke & Collins, 2011). However, with spray aeration alone, there is clearly a large discrepancy in the removal efficiency between the Cl-THMs (e.g., CHCl_3) and Br-THMs (e.g., CHCl_3).

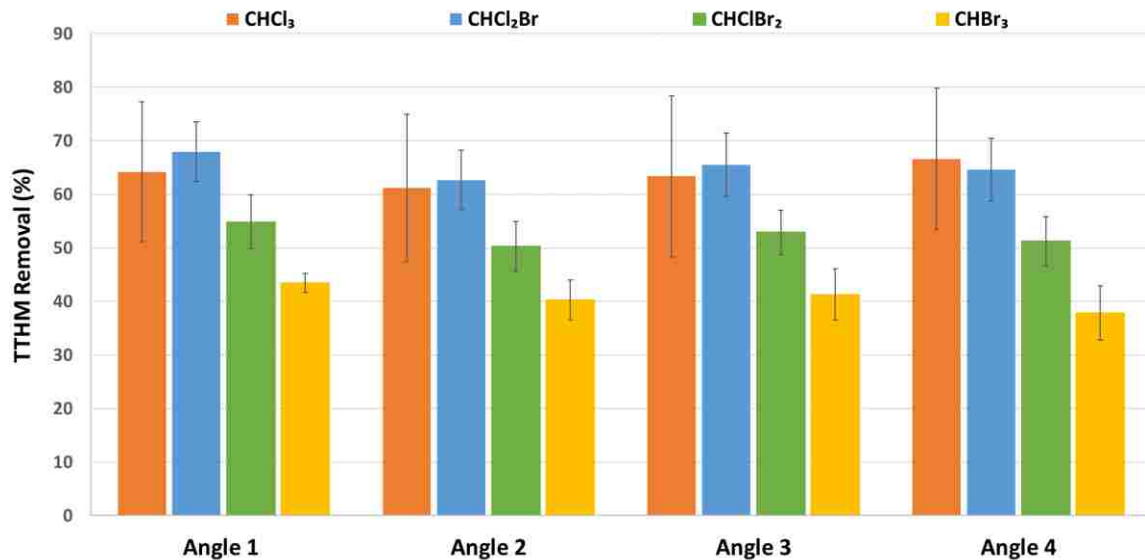


Figure 5-2 Averaged sum of formation and removal for TTHM species under different blower configurations at the same air flow rate (55 cfm) with one vent open. Formation of individual TTHM species were assumed to be equal to the averaged formation in the preliminary study of the fully enclosed tank (averaged TTHM formation $8.5 \pm 3.5\%$).

■ Blower Angle

Changing the blower angle changed TTHM removal efficiency. Angle 1 (straight down) and Angle 3 (toward the spray nozzle) produced the highest CHCl_2Br , CHClBr_2 , and CHBr_3 removal efficiencies. Angle 4 (toward the tank wall) surprisingly produced similar TTHM removal efficiencies. Angle 2 (45° from the wall) produced slightly lower removals efficiency; this was unexpected, as the model outputs indicated that this configuration helped air to circulate homogeneously in the tank. This could have been due to the fact that Angle 1, 3, and 4 provided additional mixing or turbulence from the direct contact between the fresh air and contaminated water (Roberts & Levy, 1985). This helps to reduce film thickness at the air-water interface, a parameter that was not considered in the model. Angle 2 did not provide this direct air to water contact. However, the differences in % TTHM removals between Angle 1 (best) and Angle 2 (worst) was <5%, which was not significant at the 95% confidence level based on ANOVA results ($p=0.057$). In addition, the difference in % TTHM removals among all four angles were not significant ($p=0.315$). In a previous study of diffused aeration, Bilello & Singley (1986) determined that the volume of air applied was more influential to TTHM removals than how air was applied.

Angle 3 was selected to test the other investigated variables, as this was one of the angles that provided the best TTHM removal efficiency.

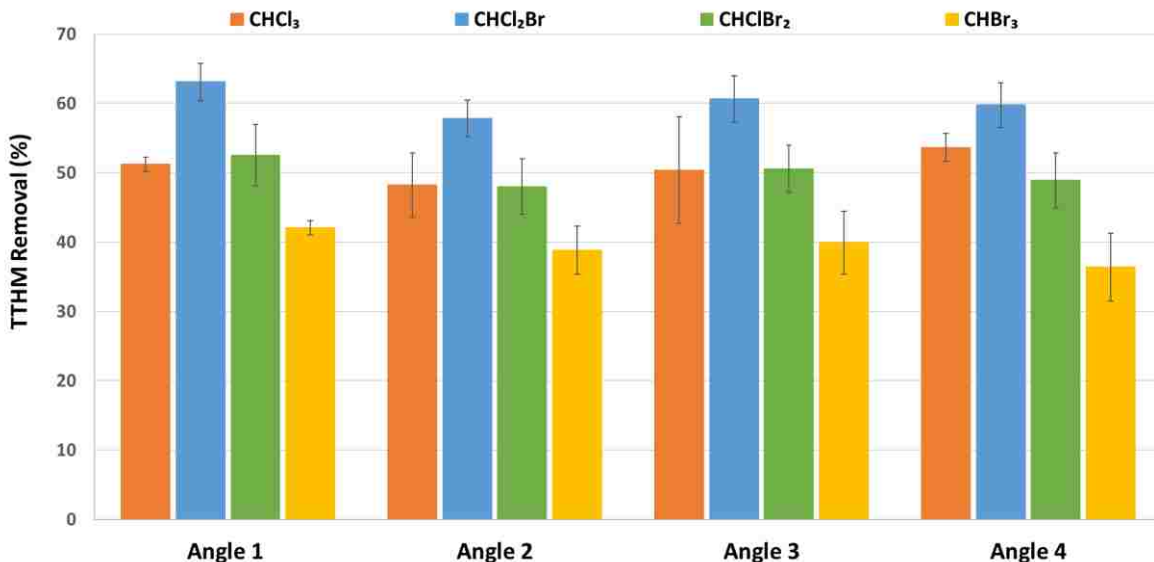


Figure 5-3 Averaged removal efficiencies for TTHM species for different blower configurations at the same air flow rate (55 cfm) with one vent open. Error bars represent one standard deviation (n=2-4).

■ Air Flow Rates

The effect of ventilation air flow rate on TTHM removals was a focus of this study. Initially, tests were conducted with the spray aeration nozzle employed in the pilot-scale tank equipped with two 6-in vents without a blower. The averaged removal efficiency for all TTHM species increased significantly ($p < 0.001$) after opening two vents compared to those of the fully enclosed tank (averaged TTHM formation $8.5 \pm 3.5\%$). Thus, the stripped THMs were able to exit the headspace through passive ventilation of 15 cfm at each vent. Installing two vents increased THM removals by 50.4% for CHCl₃, 47.9% for CHCl₂Br, 47.9% for CHClBr₂, and 33.1% for CHBr₃ (Figure 5-4). As expected, the efficiency of overall mass-transfer processes is highly influenced whether the system is properly vented or not.

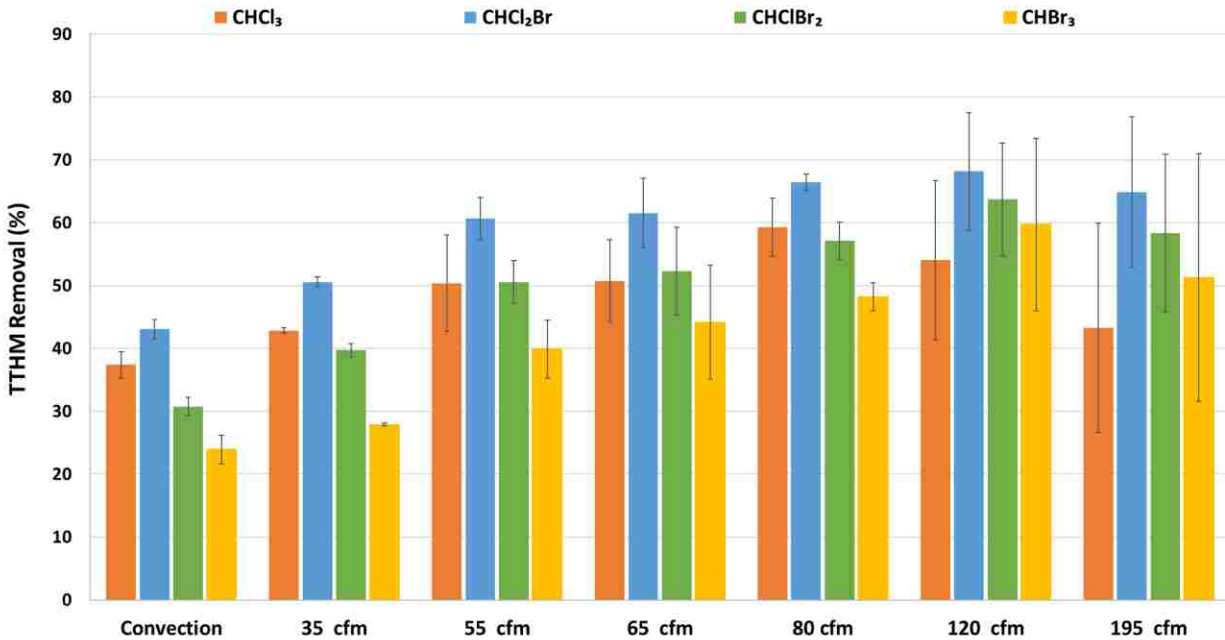


Figure 5-4 Averaged removal efficiencies for TTHM species for different blower air flow rates with the same blower configuration (Angle 3, toward the nozzle) and with one vent open, except passive ventilation, which is with two vents open. Error bars represent one standard deviation (n=2-4).

To further investigate the effects of air discharged into the system on performance, different air flow rates (35, 55, 65, 80, 135, and 195 cfm) were tested. One vent at Location A was used for these cases. Comparable to previous cases, the removal of CHCl₂Br was the highest, followed by CHCl₃, CHClBr₂, and CHBr₃, respectively. As shown on Figure 5-4, removals of all TTHM species increased with increased air flow rates. Compared to the case of passive ventilation, ventilating 35-cfm air flow rate increased removals by 5.5% for CHCl₃, 7.5% for CHCl₂Br, 9.0% for CHClBr₂, and 4.0% for CHBr₃ removals.

At lower air flow rates, the highly chlorinated-TTHMs were the most amenable to stripping. As a larger air volume or flow rate was introduced by forced ventilation, removal of the highly brominated species increased faster than removal of the chlorinated ones. Comparing to the case of passive ventilation, 80 cfm increased removals by 13.0% for CHCl₃, 17.6% for CHCl₂Br, 26.4% for CHClBr₂, and 24.3% for CHBr₃, respectively. Figure 5-5 presents the correlation

between air flow rate and % individual THM specie removal. The removal rate, represented as the slope, increased as the speciation shifted from Cl-THMs to Br-THMs. These removal rates were 0.323 for CHCl_3 , 0.366 for CHCl_2Br , 0.415 for CHClBr_2 , and 0.405 for CHBr_3 . The reason for this is that the Br-THMs are more gas film-controlled than the Cl-THMs; thus, they are more difficult to remove by aeration (Brooke & Collins, 2011). This agrees with their Henry's constant. However, as a larger air volume or flow rate was introduced by forced ventilation, the removal efficiencies of gas-film controlled THMs was more pronounced than those of liquid-film controlled THMs. Roberts & Munoz (1985) determined air flow rates have more influence on K_{La} values of gas-film controlled compounds. On the contrary, the removal efficiency of liquid-film controlled THMs (e.g., CHCl_3) are not changed as substantially when additional air flow rates exceed a threshold, mainly because the effects on their K_{La} values are independent of air flow rate. Thus, the combination of spray aeration and forced ventilation dramatically reduces the anomaly between the removal efficiencies between Cl- and Br-THMs than employing spray aeration alone. Brooke & Collins (2011) also determined this smaller discrepancy when employing spray aeration compared to diffused aeration. This outcome is preferred as Br-THMs are more toxic and difficult to remove by aeration.

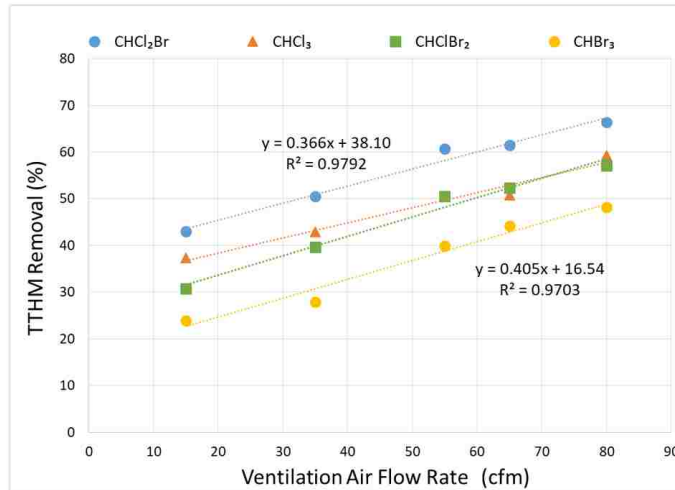


Figure 5-5 Correlations between ventilation air flow rates (0-80 cfm) and individual TTHM species removal. The rates presented are 0.366 for CHCl₂Br and 0.405 for CHBr₃.

At higher air flow rates, which included 135 cfm and 195 cfm, TTHM removals did not increase significantly ($p=0.575$). An air flow rate of 135 cfm attained higher CHCl₂Br, CHClBr₂, CHBr₃ removal efficiencies, which were 68.2%, 63.7%, and 59.7%, respectively. However, the average removal efficiency of CHCl₃ slightly decreased to 54.0%, indicating that the higher ventilation air flow did not have pronounced effect or negatively impacted CHCl₃ removal efficiency. Similarly, the 195-cfm air flow rate decreased the removal efficiency of Cl-TTHMs (i.e., CHCl₃ and CHCl₂Br). More testing is needed to ascertain if the decreases are statistically relevant, as only one experiment with two HRTs were performed for each these higher air flow rate.

Averaged TTHM removals at different blower air flow rates were statistically significantly different for 15 cfm and 35 cfm. Shown in Table 5-1, there was an interaction effect between TTHM species and blower air flow rate using a two-factor ANOVA (interaction effect, $p=0.01$).

Table 5-1 Two-factor ANOVA results between air flow rates and % TTHM removals

Source of Variation	SS	df	MS	F	P-value	F crit
Sample	5.215059	7	0.745008	137.6865	3.61E-47	2.106465
Columns	0.367129	3	0.122376	22.61659	3.69E-11	2.699393
Interaction	0.216837	21	0.010326	1.908291	0.018473	1.667034
Within	0.519447	96	0.005411			
Total	6.318472	127				

Therefore, the effect of blower air flow rates on TTHM removal was considered separately for each THM specie. The difference in CHCl_3 removals were significant at air flow rates of 15 cfm ($p < 0.001$) and 35 cfm ($p = 0.025$). The difference in CHCl_2Br and CHClBr_2 removals were significant at air flow rates of 15 cfm ($p < 0.001$), 35 cfm ($p < 0.003$) and 55 cfm ($p < 0.016$). The difference in CHBr_3 removals were significant at air flow rates of 15 cfm ($p < 0.001$) and 55 cfm ($p = 0.025$). Overall, the higher air flow rates, > 55 cfm, produced averaged removals that were not statistically significant with 95% confidence level.

■ Vent Location

In storage reservoirs, it is important to consider the effects of vent location on TTHM removal efficiency by spray aeration. Three locations were tested: Location A at the outer edge of the tank close to the blower, Location B in the center of the tank, and Location C at the outer edge of the tank opposite of the blower. To relieve air pressure from building up in the tank, tanks are typically equipped with at least one vent near the center of the tank (AWWA, 1997). However, as can be seen on Figure 5-6, this placement (Location B) produced the lowest TTHM removal efficiency, especially for CHBr_3 . Changing from vent Location B to Location C increased THM removal but the change was not statistically significant even for CHBr_3 removals ($p = 0.057$). An explanation for this result may due to the fact that spray nozzle was also located near the center of

the tank. As shown in the model, the water droplets were being sprayed at a relatively higher flow rate than the air; thus, the droplets had more momentum to influence the path of the air molecules. Additionally, these droplets could also easily obstruct the contaminated air from exiting through the vent, which was located next to the nozzle itself. Secondly, Location B also generated the least homogeneous air circulation in the model, subsequently causing dead spots in the headspace that may negatively impact performance.

Locating the vent at the outer edge of the tank (Location C) or closer to blower (Location A) allows the air to exit the headspace without any obstruction after coming into contact with the droplets. This helps when the duct tube directs the air into the tank as opposed to having the air discharged at the top of the tank. In the latter case, the air may easily leave through the nearby vent without much contact with the droplets. However, additional studies may be needed to test this.

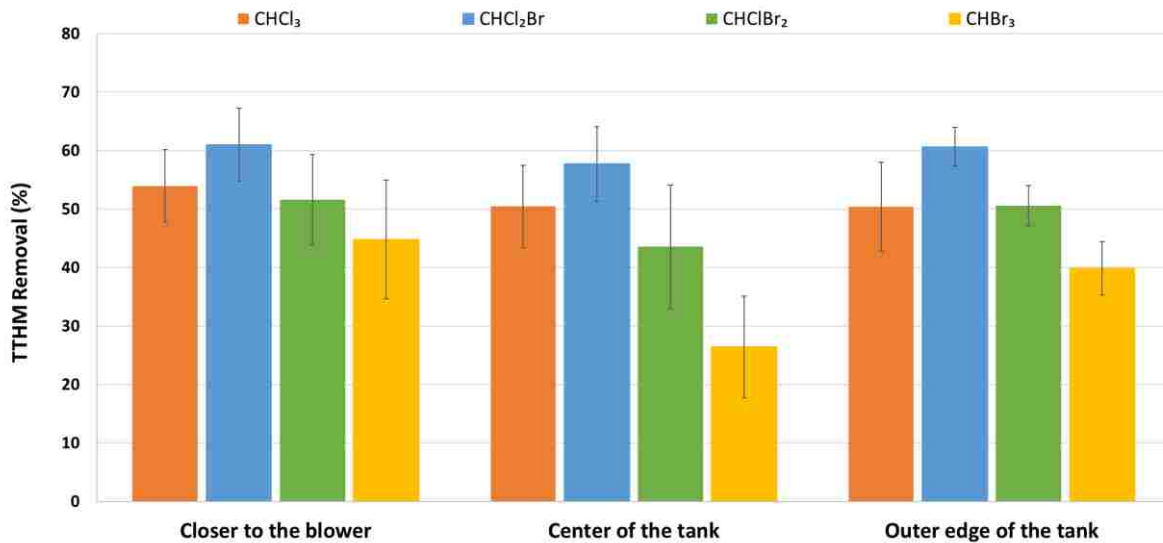


Figure 5-6 Averaged removal efficiencies for TTHM species at different vent placements with the same blower air flow rate (55 cfm) and configuration (Angle 3, toward the nozzle). Error bars represent one standard deviation (n=2-4).

■ Number of Vents

The effect of number of vents on TTHM removal efficiency was investigated. The removals of all species appear to be relatively the same for 1, 2, and 3 vents (Figure 5-7). ANOVA indicates installing one vent is significant to all TTHM species ($p < 0.001$) compared to no vents. However, more than one vent (i.e., two or three) did not provide a significant increase in TTHM removal efficiency ($p = 0.688$) compared to one vent. Thus, adding at least one vent in this pilot-scale tank allowed contaminated air to exit the system, but additional vents do not insignificantly increase TTHM removals.

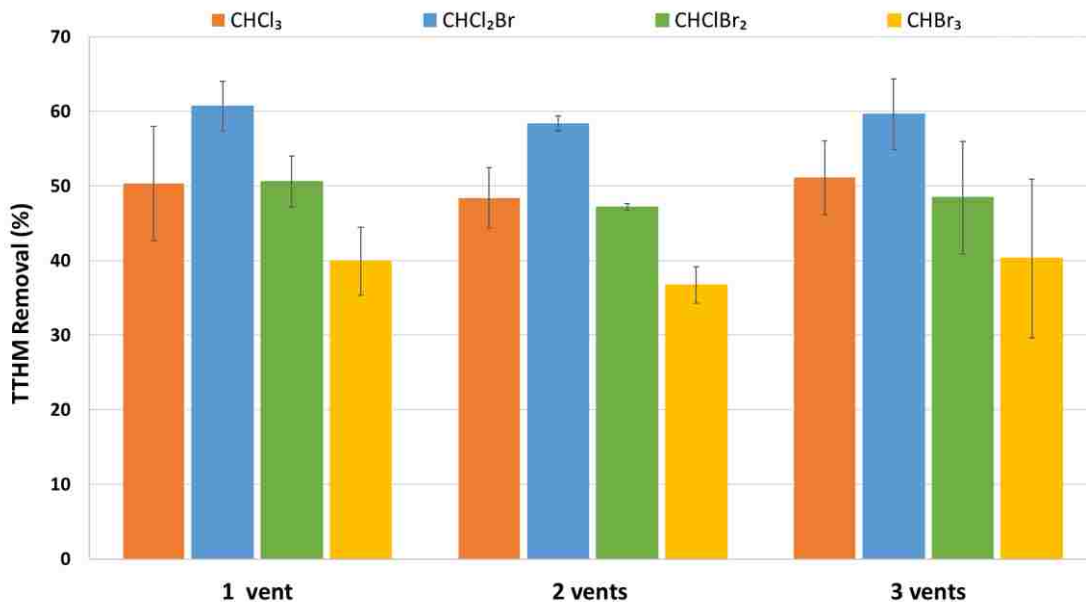


Figure 5-7 Averaged removal efficiencies for TTHM species with a different number of vents at the same air flow rate (55 cfm) and blower configuration (Angle 3, toward the nozzle). Error bars represent one standard deviation (n=2-4).

■ ANOVA Results

Although trends appeared for air flow rates, blower angle, and vent location, 1-way factor ANOVA results indicate that their effects on TTHM removals are not all significant with 95% confidence level (Table 5-2). The only significantly different air flow rates for THM species

removal efficiency were 15, 35, and 55 cfm. Lastly, increasing the number of vents from 0 to 1 produced significantly different removals of individual THMs species; however additional vents >1 did not produced significant removals. Blower angle and vent location produced removals that were not significantly improved based on 95% confidence. Additional ANOVA results are included in Appendix A. Potential explanations for these results are that other experimental variables were not sufficiently controlled (e.g., influent THMs concentration or temperature) because this pilot-scale experiment were conducted outside, where external influences could not be well controlled.

Table 5-2 ANOVA results for the significance of each parameter on THM removal efficiency. Y represents significant ($p < 0.05$) and N represents not significant ($p > 0.05$).

Variable	Comparison	CHCl ₃	CHCl ₂ Br	CHClBr ₂	CHBr ₃	Adjusted TTHM
Blower flow rate	0, passive ventilation (15 cfm)	Y	Y	Y	Y	Y
	15, 35	Y	Y	Y	N	Y
	35, 55	N	Y	Y	Y	N
	55, 65	N	N	N	N	N
	65, 80	N	N	N	N	N
	80, 135	N	N	N	N	N
	135, 195	N	N	N	N	N
Blower angle	1, 2	N	N	N	N	N
	2, 3	N	N	N	N	N
	3, 4	N	N	N	N	N
Vent location	A, B	N	N	N	N	N
	B, C	N	N	N	N	N
	A, C	N	N	N	N	N
Number of vents	0, 1	Y	Y	Y	Y	Y
	1, 2	N	N	N	N	N
	2, 3	N	N	N	N	N

Water Quality and Air Conditions

Monitored water quality parameters were water temperature, pH, conductivity, and concentrations of TOC, bromide, and free chlorine residual. Monitored air conditions were air flow rates, air temperature, and RH. Statistical analyses with paired-samples Student's t-test for

paired samples were conducted for each parameter to identify the statistical significance of these parameters between the inlet and outlet water samples with 95% confidence level. In addition, analysis was conducted to identify any correlation between each parameter and % TTHM removal.

Water quality

Table 5-3 summarizes the averaged results for water temperature, pH, conductivity, and concentrations of TOC, bromide, and free chlorine residual between the inlet and outlet water samples.

Table 5-3 Monitored averaged water quality results for all experiments.

Sample Type	Water Temperature (°C)	pH	Conductivity (µS/cm)	TOC (mg/L)	Bromide (mg/L)	Free Chlorine Residual (mg/L)
Inlet	18.7 ± 0.4	7.53 ± 0.11	1104 ± 48	2.50 ± 0.43	0.313 ± 0.065	1.25 ± 0.11
Outlet	19.0 ± 0.5	7.87 ± 0.13	1099 ± 60	2.55 ± 0.52	0.394 ± 0.053	1.00 ± 0.14

Results from the paired t-tests show that pH change between inlet and outlet water samples is statistically significant ($p < 0.001$). An explanation for this is that employing spray aeration, especially with forced ventilation, strips the CO_2 , which has an $H_c = 1.22$ (Sander, 2015), from the water, increasing the pH. This was also identified in a previous study, in which the pH increase ranged from 0.15-0.2 pH units (Clark, 2016).

Due to the pilot-scale tank being placed outside to simulate field conditions, water temperature statistically varied significantly ($p < 0.001$) between inlet and outlet water samples. This is due to the contact between the cooler water and warmer air, which slightly increased the temperature of the water in the tank during the endothermic interaction. This is natural

consequence is also discussed in the air conditions section, which provides an explanation for the decrease in air temperature between the entrance and exit of the tank.

Bromide concentration may affect the speciation, TTHM removals by spray aeration, and post-treatment THMFP. The measured bromide concentrations include both inorganic and organic bromide (e.g. Br-THMs). This parameter statistically varied significantly between inlet and outlet water samples. An initial explanation for this difference may have been due to water evaporation as a result of employing ventilation and spray aeration. Additionally, since inorganics (e.g., Br⁻) are not efficiently removed by spray aeration, high evaporation rates can decrease the volume of water without changing the mass of Br⁻ ions, subsequently, increasing the concentration of Br⁻ in the system compared to the inlet water. However, evaporation calculations of the system with 80-cfm air flow rate in Appendix A showed that the evaporation rates with 80 cfm air flow rate were very small (<1%), which could not explain the increase in Br⁻ concentration.

Chlorine concentration is an important parameter to monitor in drinking water because the US EPA requires a free chlorine residual concentration of 0.2 mg/L to be maintained in the distribution system (Sander, 2015). Free chlorine concentration statistically varies significantly between inlet and outlet water samples. However, employing vents and/or forced ventilation produced very little to negligible losses of chlorine compared to the fully enclosed tank system (Table 5-4). This indicates that the loss of free chlorine residual was mainly due to reaction between the free chlorine residual and precursors (e.g., TOC and Br⁻) in the water pool. Spray aeration is not an effective technique to remove these precursors or natural organic matters.

Table 5-4. Percent drop in averaged chlorine concentrations for each air flow.

Air flow rates (cfm)	0 ⁽¹⁾	15 ⁽²⁾	35	65	80	135	195
Drop (%)	16.7 ± 5.3	20.2 ± 5.9	23.3 ± 0.2	23.1 ± 7.0	24.3 ± 3.7	16.7 ± 8.6	24.9 ± 4.4

⁽¹⁾ Fully enclosed tank; ⁽²⁾ passive ventilation with two open vents

Conductivity and TOC were monitored to ensure water quality was stable for all experiments and was not expected to be affected by spray aeration. Due to issues with the TOC analyzer, TOC concentrations were not monitored for all experiments; thus, only runs where TOC was measured were used in this analysis. Conductivity and TOC concentrations between the inlet and outlet water samples did not statistically vary significantly ($p>0.33$).

■ Air Conditions

Table 5-5 summarizes the averaged results for flow rates, air temperature, and RH between the inlet (blower) and outlet (vent).

Table 5-5 Monitored averaged air conditions for all experiments.

Location	Air flow (cfm)	Air Temperature (°C)	Relative Humidity
Inlet (blower)	58.53 ± 41.50	27.99 ± 2.07	18.9 ± 4.3
Outlet (vent)	56.11 ± 37.23	24.00 ± 2.05	77.7 ± 12.0

Air flow rate ($p=0.006$), air temperature ($p<0.0001$), and RH ($p<0.0001$) statistically vary significantly between the blower and vent. As air is ventilated into the tank, it comes into contact with the water droplets, which have a lower temperature. The air temperature would then drop since water evaporates, which is a natural consequence of humidification. This is also shown with the high difference in humidity between the outlet and inlet measurements. Additionally, this consequence would also explain the slight decrease in air velocity between the entrance and exit. The reason for this result is that the water is also escaping with the air, thereby, slowing the speed of the gas in the tank. Additional water quality results for each experiment are included in Appendix A.

Correlations

All water quality and air conditions parameters and inlet TTHM concentrations were analyzed for potential correlations with % TTHM removals. Figure 5-8 presents the relationship, along with the R^2 values between temperature and initial free chlorine residual levels and % TTHM removals. The coefficient of determination for the tested inlet air flow rates and % TTHM removals was 0.253, which was the highest among all parameters. The coefficient of determination for inlet free chlorine residual levels and % TTHM removals was 0.067, indicating no correlation. The graphs and R^2 values for the other parameters are included in Appendix A. Overall, other R^2 values between each parameter and % TTHM removal were all less than 0.146. Thus, these water quality and air conditions parameters were not correlated to TTHM removals. Correlation graphs with R^2 values for other parameters are included in Appendix A.

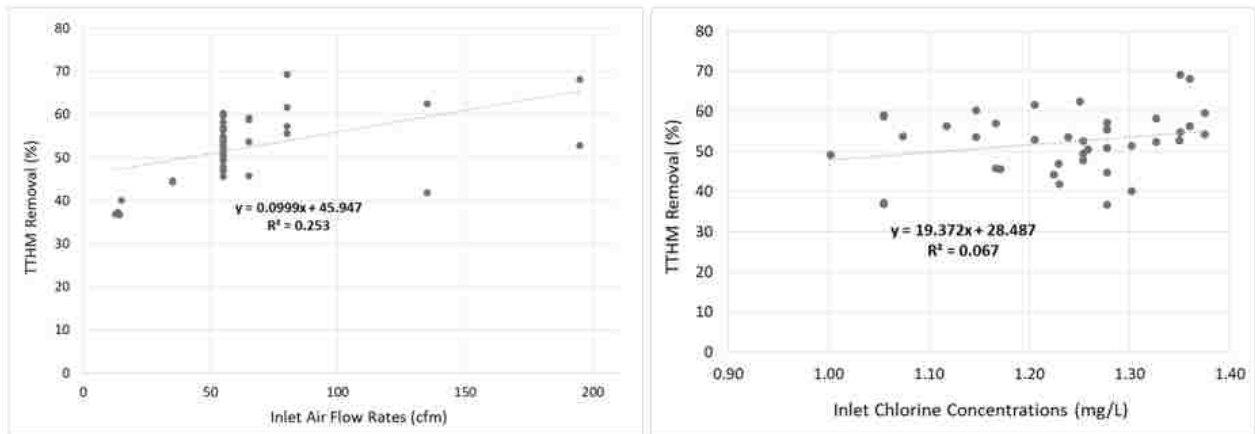


Figure 5-8 Correlations between inlet conditions and % TTHM removals.

Chapter 6 — Conclusions and Recommendations

The difficulty of conventional treatments to remove bromide and organic precursors—such as DOM— may result in TTHM levels in the distribution system exceeding the MCLs established by the USEPA Stage 1 and 2 DBPR. Thus, a suitable and viable treatment option is spray aeration, which can be employed in the distribution system (e.g., storage tanks) to meet the regulations in problematic areas. Spray aeration was found to be effective in removing VOCs such as THMs through a mass-transfer process. Evacuating the headspace in the tank becomes crucial because otherwise these contaminants coalesce and re-contaminate the water. However, there is a lack of research on the performance of spray aeration in a relatively enclosed storage tank vented to the atmosphere. With a pilot-scale tank employed with a spray aerator, different headspace ventilation variables were investigated to analyze their effects on the removal of individual TTHM species.

Conclusions based on the results of this study are given below:

- Spray aeration is highly effective in removing TTHM; however, proper ventilation is required in relatively enclosed systems (e.g., storage tanks) to enhance THMs removals. Preliminary studies with a fully enclosed pilot-scale tank resulted in TTHM formation, although the water was being treated by the spray aeration. The overall averaged TTHM formation was $8.5 \pm 3.5\%$, such that formation of CHCl_3 was the highest, followed by CHCl_2Br , CHClBr_2 , and CHBr_3 , respectively. This was attributed to the reaction between the free chlorine residual and precursors in the water that dropped free chlorine residual levels by $16.5 \pm 5.3\%$.
- Air flow rate substantially increased TTHM removal efficiency in a relatively enclosed tank. Increasing air flow rates proportionally increased TTHM removal efficiency. Opening two vents (15 cfm of passive ventilation) attained removal of 50.4% for CHCl_3 , 47.9% for

CHCl₂Br, 47.9% for CHClBr₂, and 33.1% for CHBr₃. When discharging 80 cfm in the relatively enclosed pilot-scale tank equipped with one vent, the overall removals increased by 21.9%, 23.4%, 26.4%, and 24.3%, respectively. More experiments are needed to confirm whether or not TTHM removal plateaus above 80 cfm, which represents an air-to-water ratio of 200:1. This finding indicates that it is worthwhile to optimize air flow rates for ventilation in real. Lastly, as air flow rate increased, the rate of increase for Br-THM removal exceeded the rate of increase for Cl-THMs removal.

- Trends indicate that Angle 2 produced the lowest TTHM, but blower angle did not produce significant TTHM removal. The highest difference in TTHM removal among the four investigated blower angles was <5%, indicating that angle blower has little effect on removals. Thus, increasing the volume of air is more important than the way it is applied. However, this finding was not as expected based on the model results, which show that Angle 2 induces the best homogenous air flow around the headspace. Limitations of these simulations were neglecting THM formation and mass-transfer coefficients since this model was used as a preliminary source for experimental work.
- Trends indicate that placing the vent near the spray nozzle resulted in the lowest TTHM removal efficiency, but vent location did not produce significant TTHM removals. Placing the vent near the center of the tank resulted in the lowest TTHM removal efficiency because the water droplets hindered the contaminated air from leaving through the vent. This was in agreement with the model results, which show that this placement induced more dead spots within the headspace and no air stream path appeared to exit through the vent. However, changing the vent location did not have a significant influence on TTHM removal efficiency.

- Installing 1 vent produced significant TTHM removal efficiency, but numerous vents (>1 in this study) produced insignificant TTHM removals. It is necessary to have at least one vent installed in the tank so that the air contaminated with stripped THMs can exit the headspace through them. However, >1 vent did not significantly increase TTHM removals because it is relatively easy for air to be released into the atmosphere.
- Monitored inlet TTHM concentrations, water quality parameters, and air conditions did not have strong correlation with % TTHM removals. The R^2 value between air flow rate and TTHM removals was 0.236, which was the highest among the monitored parameters. The other R^2 values of the other parameters and TTHM removals were <0.134.
- Free chlorine residual concentrations did not seem to be reduced by aeration, but it did drop mainly due to formation with precursors in the water pool. The inlet and outlet free chlorine residual levels statistically varied significantly; however, the % drop in removals for all experiments were relatively similar to that of the enclosed tank, indicating that most of the drop was mainly attributed to reaction with precursors in the water.

Due to the lack of study of spray aeration in a relatively enclosed tank, more studies on spray aeration should be conducted in a closed system vented to the atmosphere.

Recommendations for future work are provided below:

- A study in a relatively enclosed tank that evaluated the effects of air flow rates and other variables (e.g., nozzle heights or recycle flows) that have been shown to influence TTHM removals.
- Due to relatively high standard deviations, additional follow-up studies is needed to confirm the results for the higher air flow rates (e.g., 120, 195 cfm).

- A repeat study at different times of the year to determine the effect of air temperature on TTHM removals.
- A study without the presence of the duct tube, which directs the air flow, as this component is typically not used in full-size reservoirs. In addition, the effects of vent location due to this change should be investigated.
- A parallel study comparing effects of air flow rates and vent locations for spray aeration and surface aeration, which is also widely employed. In addition, a comparison is needed to compare power inputs and water evaporation losses for the two approaches, so that the cost per unit mass of TTHM removed can be compared along with performance (actual removals obtained by each system).
- A study comparing the energy required for forced ventilation and amount of TTHM removal efficiency for spray and surface aeration.
- Further optimization of the CFD model, which needs to consider the mass transfer coefficients of THM species between the headspace and water droplets in the relatively enclosed tank. The CFD model should be run without the duct tube, and also scaled up to a full size underground reservoir headspace.

Appendix A

Averaged water quality parameters for each experiment.

Test Date	Sample Type	pH		Water Temperature (°C)		Conductivity (µS/cm)		Chlorine (mg/L)		TOC (mg/L)		Bromide (mg/L)	
		In	Out	In	Out	In	Out	In	Out	In	Out	In	Out
5/13/19	Fully enclosed tank	7.5	7.6	19.0	19.6	1108	1108	1.38	1.16	2.81	2.69	0.200	0.431
		7.5	7.6	18.5	18.6	1108	1152	1.46	1.17	2.72	2.80	0.238	0.489
5/15/19		7.4	7.5	18.9	19.5	1108	1108	1.37	1.08	2.25	2.49	0.219	0.385
7.5		7.6	18.4	18.6	1108	1152	1.39	1.26	2.45	2.47	0.258	0.431	
6/3/19	Passive ventilation (15 cfm) ⁽¹⁾	7.4	7.8	18.8	19.4	1068	1064	1.05	0.78	2.29	2.29	0.203	0.424
6/7/19		7.5	7.8	18.5	19.0	1108	1008	1.05	0.91	2.30	2.33	0.427	0.435
		7.6	7.8	18.8	19.4	1068	1064	1.28	0.96	3.95	4.28	0.242	0.462
		7.6	7.9	18.5	19.0	1108	1008	1.30	1.08	2.41	2.43	0.350	0.397
6/8/19	Angle 3—80 cfm	7.6	7.8	19.8	20.0	1108	1152	1.28	0.94	2.26	2.28	0.398	0.323
		7.6	8.0	18.9	19.3	1108	1152	1.35	0.99	2.32	2.34	0.277	0.354
6/9/19	Angle 1—55 cfm	7.4	7.8	18.9	18.8	1108	1172	1.07	0.76	2.31	2.35	0.315	0.385
		7.3	7.7	18.5	18.6	1172	1152	1.15	0.88	2.41	2.43	0.393	0.470
6/11/19	Angle 2—55 cfm	7.7	8.0	18.3	19.3	1068	1028	1.26	0.87	2.25	2.30	0.308	0.327
		7.7	7.9	18.1	19.0	1008	1028	1.25	0.96	2.25	2.27	0.304	0.315
6/18/19	Angle 3—65 cfm	7.6	8.0	18.5	18.7	1048	1152	1.23	0.98	-	-	0.203	0.424
		7.6	8.0	18.5	18.7	1172	1152	1.30	1.00	-	-	0.427	0.435
6/20/19	Angle 3—195 cfm	7.5	8.0	18.6	18.7	1048	1068	1.35	0.97	-	-	-	-
		7.5	8.0	18.2	18.3	1048	1048	1.36	1.06	-	-	-	-
6/22/19	Angle 3—135 cfm	7.5	7.9	18.5	19.0	1068	1048	1.25	0.97	-	-	-	-
		7.5	8.0	18.5	18.6	1048	1028	1.23	1.10	-	-	-	-
6/23/19	Angle 3—65 cfm	7.4	7.8	18.8	18.9	1068	1028	1.05	0.78	-	-	0.308	0.261
		7.3	7.8	18.5	18.7	1008	1028	1.05	0.91	-	-	0.315	0.373
6/24/19	Angle 3—55 cfm	7.4	7.8	18.9	19.4	1152	1168	1.23	0.94	-	-	0.366	0.431
		7.5	7.9	18.3	18.4	1152	1028	1.25	0.99	-	-	0.354	0.393
6/24/19	Two vents—55 cfm ⁽²⁾	7.4	7.8	18.9	19.4	1068	1064	1.21	0.91	-	-	0.242	0.412
		7.6	7.9	18.3	18.4	1108	1008	1.25	1.04	-	-	0.431	0.470
6/25/19	Three vents—55 cfm	7.6	8.0	19.2	19.8	1152	1168	1.17	0.85	-	-	0.354	0.393
		7.6	8.0	18.5	18.7	1152	1084	1.00	0.71	-	-	0.315	0.431
6/26/19	Angle 1—55 cfm	7.6	7.9	19.0	19.4	1048	1168	1.33	1.18	-	-	0.339	0.373
		7.7	7.9	18.6	18.7	1152	1084	1.35	1.21	-	-	0.373	0.451
6/28/19	Angle 3—35 cfm	7.4	7.8	18.9	19.4	1152	1168	1.22	0.94	-	-	0.366	0.431
		7.5	7.9	18.3	18.4	1152	1028	1.28	0.98	-	-	0.354	0.420
6/28/19	Angle 3—	7.4	7.8	19.4	20.1	1152	1168	1.35	1.11	-	-	0.319	0.431

	55 cfm	7.5	7.9	19.2	19.3	1152	1028	1.37	1.18	-	-	0.331	0.451
6/29/19	Angle 3— 80 cfm	7.6	7.9	18.9	19.4	1048	1168	1.21	0.91	-	-	0.373	0.381
		7.7	7.9	18.4	18.7	1048	1084	1.28	1.04	-	-	0.381	0.431
6/29/19	Angle 2— 55 cfm	7.5	7.8	18.4	18.4	1152	1168	1.30	1.13	-	-	0.258	0.323
		7.6	8.0	18.1	18.3	1152	1152	1.37	1.18	-	-	0.277	0.354
6/18/19	Angle 4— 55 cfm	7.5	7.9	18.6	19.2	1048	1168	1.33	1.12	-	-	0.315	0.325
		7.5	8.0	18.5	18.6	1048	1168	1.36	1.25	-	-	0.318	0.321
6/30/19	Closer vent— 55 cfm	7.7	8.0	19.0	20.0	1152	1084	1.15	0.94	-	-	0.258	0.323
		7.7	7.9	18.5	18.8	1152	1084	1.28	1.06	-	-	0.277	0.354
6/30/19	Middle vent— 55 cfm	7.5	8.0	18.3	19.3	1152	1168	1.17	0.93	-	-	0.215	0.381
		7.7	7.9	18.1	19.0	1152	1028	1.12	0.83	-	-	0.315	0.369

⁽¹⁾ Vent Location A and C; ⁽²⁾ Vent Location B and C

Air flow conditions for each experiment

Test Date	Sample Type	Air Flow (cfm)		Air Temperature (°C)		Relative Humidity	
		In	Out	In	Out	In	Out
5/13/19	Fully enclosed tank	0	0	-	-	-	-
		0	0	-	-	-	-
5/15/19		0	0	-	-	-	-
		0	0	-	-	-	-
6/3/19	Passive ventilation (15 cfm) ⁽¹⁾	13.5	25.2	25.3	24.9	27.6	76.5
		12.6	25.1	24.3	23.6	20.7	76.5
6/7/19		14.1	23.0	24.4	23.4	27.6	78.6
		14.9	24.0	24.3	22.7	20.7	78.6
6/8/19	Angle 3—80 cfm	80.0	76.4	28.0	22.5	10.5	87.5
		80.0	78.3	27.4	21.3	10.5	92.6
6/9/19	Angle 1—55 cfm	55.0	53.1	27.7	23.0	19.0	89.4
		55.0	50.4	26.8	21.8	22.3	92.8
6/11/19	Angle 2—55 cfm	55.0	51.3	29.0	24.6	19.5	62.8
		55.0	52.0	26.3	24.5	21.6	67.4
6/18/19	Angle 3—65 cfm	65.0	61.5	30.1	23.4	12.6	82.6
		65.0	62.4	26.7	22.6	17.5	86.4
6/20/19	Angle 3—195 cfm	195.0	180.0	26.3	24.7	19.6	86.5
		195.0	175.0	24.3	22.0	23.2	87.4
6/22/19	Angle 3—135 cfm	135.0	125.0	27.5	25.4	18.9	84.4
		135.0	123.5	25.7	23.6	21.5	86.4
6/23/19	Angle 3—65 cfm	65.0	61.5	29.2	23.0	22.3	86.5
		65.0	62.4	28.1	22.1	23.0	87.9
6/24/19	Angle 3—55 cfm	55.0	53.1	28.0	24.2	19.0	83.1
		55.0	50.4	27.4	23.7	22.3	83.6
6/24/19	Two vents—55 cfm ⁽²⁾	55.0	49.7	29.0	28.4	13.5	56.0
		55.0	45.8	26.1	23.8	10.4	63.5
6/25/19	Three vents—55 cfm	55.0	63.3	31.0	28.7	16.5	46.3
		55.0	67.1	30.4	27.9	18.3	42.9
6/26/19	Angle 1—55 cfm	55.0	53.3	30.5	25.2	19.0	85.4
		55.0	50.4	29.7	20.6	23.6	89.7
6/28/19	Angle 3—35 cfm	35.0	32.8	30.1	25.9	23.6	77.6
		35.0	32.2	26.7	22.9	18.6	79.8
6/28/19	Angle 3—55 cfm	55.0	53.1	29.1	24.7	19.0	85.4
		55.0	50.4	27.4	22.6	22.3	85.6
6/29/19	Angle 3—80 cfm	80.0	77.3	28.0	22.0	10.5	93.8
		80.0	76.2	27.4	20.6	14.9	66.8

6/29/19	Angle 2—55 cfm	55.0	50.1	28.0	24.2	19.0	63.8
		55.0	50.4	27.4	23.7	19.7	68.9
6/18/19	Angle 4—55 cfm	55.0	50.1	29.4	26.4	17.8	74.6
		55.0	51.2	28.4	24.5	18.4	79.5
6/30/19	Closer vent—55 cfm	55.0	52.3	30.4	23.2	15.8	69.8
		35.0	50.4	32.3	22.5	14.8	70.6
6/30/19	Middle vent—55 cfm	55.0	50.2	32.3	28.7	19.6	75.6
		55.0	50.4	29.4	26.8	19.5	76.5

(¹) Vent Location A and C; (²) Vent Location B and C

Averaged inlet and outlet concentrations of individual species and TTHM for each experiment

Test Date	Sample Type	CHCl ₃ (µg/L)		CHCl ₂ Br (µg/L)		CHClBr ₂ (µg/L)		CHBr ₃ (µg/L)		Adjusted TTHM (µg/L)	
		In	Out	In	Out	In	Out	In	Out	In	Out
5/13/19	Fully enclosed tank	23.15	26.92	19.40	20.14	12.73	12.53	2.20	2.17	45.62	49.80
		21.05	25.08	17.75	19.53	12.02	12.20	2.10	2.16	41.86	47.32
5/15/19		14.30	15.57	10.75	11.20	7.28	7.72	1.53	1.54	27.03	28.88
		22.12	23.78	17.66	17.91	11.20	11.57	2.16	2.24	42.42	44.52
6/3/19	Passive ventilation (15 cfm) ⁽¹⁾	23.48	15.09	21.81	12.33	15.65	10.62	2.28	1.71	49.41	30.97
6/7/19		28.55	18.14	24.24	14.01	16.91	11.84	2.80	2.14	57.23	36.15
		27.80	17.54	26.45	15.47	17.50	12.41	2.84	2.25	58.44	36.98
		28.03	16.70	25.53	14.05	17.22	11.74	2.91	2.15	57.87	34.68
6/8/19	Angle 3—80 cfm	32.50	14.75	30.35	11.79	18.57	9.46	3.15	1.91	66.74	29.66
		33.56	12.01	29.51	6.97	18.98	5.60	3.20	0.98	67.44	20.76
6/9/19	Angle 1—55 cfm	31.75	15.49	28.95	11.48	19.62	9.75	3.21	1.83	65.60	30.31
		32.73	16.42	29.46	11.17	19.22	9.73	3.23	1.84	66.73	31.00
6/11/19	Angle 2—55 cfm	33.86	18.35	29.60	12.10	19.21	9.76	3.29	1.92	67.99	33.67
		32.98	18.78	28.86	12.51	18.79	10.09	3.19	1.99	66.28	34.62
6/18/19	Angle 3—65 cfm	22.74	13.02	20.65	9.61	15.26	8.85	2.10	1.45	47.52	25.78
		24.77	12.88	22.65	8.53	16.67	7.66	2.19	1.20	51.86	24.05
6/20/19	Angle 3—195 cfm	18.32	8.24	14.00	3.74	9.80	3.22	1.21	0.42	34.71	13.01
		18.12	12.41	13.98	6.10	9.93	5.02	1.27	0.80	34.59	20.11
6/22/19	Angle 3—135 cfm	18.49	10.16	16.95	6.51	13.35	5.70	1.81	0.90	39.34	18.59
		24.52	9.08	22.07	5.58	16.92	5.07	2.65	0.81	51.55	16.43
6/23/19	Angle 3—65 cfm	25.01	10.87	23.18	8.03	16.33	7.16	2.39	1.21	52.39	21.40
		24.14	10.69	22.18	7.79	17.00	7.32	2.60	1.28	51.28	21.17
6/24/19	Angle 3—55 cfm	18.30	10.64	17.36	7.58	13.58	7.40	1.85	1.23	39.61	20.99
		20.17	10.66	18.86	7.24	14.66	7.00	2.02	1.14	43.26	20.49
6/24/19	Two vents—55 cfm ⁽²⁾	27.30	13.31	26.17	10.71	18.14	9.53	2.58	1.59	57.99	27.33
		25.18	13.71	23.63	10.01	17.36	9.23	2.39	1.56	53.48	27.03
6/25/19	Three vents—55 cfm	24.65	11.19	24.61	9.12	18.64	8.62	2.88	1.50	54.62	23.49
		25.91	13.57	23.04	10.08	16.03	9.12	2.41	1.62	53.02	26.90
6/26/19	Angle 1—55 cfm	20.04	9.57	20.65	6.86	15.78	6.46	1.97	1.16	45.06	18.82
		19.82	9.58	17.33	6.39	13.44	6.55	2.02	1.19	41.10	18.55
6/28/19	Angle 3—35 cfm	15.98	9.18	16.24	8.12	12.32	7.33	1.51	1.09	35.58	19.82
		16.38	9.31	17.30	8.46	13.05	7.97	1.62	1.17	37.23	20.60
6/28/19	Angle 3—55 cfm	17.59	8.31	18.45	7.31	14.37	6.97	2.04	1.23	40.23	18.21
		19.50	7.85	20.44	7.29	14.28	6.72	2.01	1.15	43.52	17.56

6/29/19	Angle 3— 80 cfm	18.97	7.14	20.15	7.06	15.26	6.62	2.01	1.13	43.35	16.61
		18.57	8.21	17.08	6.30	12.63	6.01	1.66	0.99	39.03	16.70
6/29/19	Angle 2— 55 cfm	17.84	8.36	16.42	7.43	12.48	7.05	1.77	1.16	37.79	18.36
		18.54	9.10	19.37	7.60	15.15	7.15	2.05	1.19	42.30	19.30
6/18/19	Angle 4— 55 cfm	20.04	9.57	20.65	8.78	15.78	8.5	1.97	1.32	45.06	21.46
		20.28	9.11	20.91	7.94	16.2	7.83	1.98	1.19	45.73	19.95
6/30/19	Closer vent— 55 cfm	26.36	10.99	24.54	8.49	17.47	7.50	2.43	1.17	55.40	22.02
		23.35	11.78	22.40	9.73	16.34	8.81	2.26	1.41	50.10	24.58
6/30/19	Middle vent— 55 cfm	20.04	10.93	19.40	9.08	14.62	9.35	2.06	1.64	43.53	23.68
		22.76	10.15	21.09	7.97	14.74	7.23	2.10	1.42	47.57	20.76

⁽¹⁾ Vent Location A and C; ⁽²⁾ Vent Location B and C

Averaged removal efficiency of individual species and TTHM for each experiment

Test Date	Sample Type	CHCl ₃	CHCl ₂ Br	CHClBr ₂	CHBr ₃	Adjusted TTHM
5/13/19	Fully enclosed tank	-16.29%	-3.83%	1.61%	1.50%	-9.20%
		-19.16%	-10.04%	-1.56%	-2.86%	-13.10%
5/15/19		-8.94%	-4.11%	-6.01%	-0.98%	-6.90%
		-7.52%	-1.45%	-3.30%	-3.30%	-4.90%
6/3/19	Passive ventilation (15 cfm) ⁽¹⁾	35.74%	43.47%	32.12%	25.07%	37.30%
		36.46%	42.22%	29.99%	23.47%	36.80%
6/7/19		36.92%	41.53%	29.07%	20.85%	36.70%
		40.41%	44.97%	31.84%	26.20%	40.10%
6/8/19	Angle 3—80 cfm	54.63%	61.14%	49.07%	39.15%	55.60%
		64.20%	76.38%	70.51%	69.39%	69.20%
6/9/19	Angle 1—55 cfm	51.20%	60.36%	50.32%	42.96%	53.80%
		49.83%	62.08%	49.41%	42.91%	53.50%
6/11/19	Angle 2—55 cfm	45.82%	59.11%	49.21%	41.56%	50.50%
		43.05%	56.67%	46.31%	37.43%	47.80%
6/18/19	Angle 3—65 cfm	42.75%	53.45%	42.02%	31.04%	45.8%
		48.00%	62.35%	54.06%	45.09%	53.6%
6/20/19	Angle 3—195 cfm	55.03%	73.32%	67.17%	65.21%	62.50%
		31.49%	56.41%	49.42%	37.37%	41.90%
6/22/19	Angle 3—135 cfm	45.07%	61.57%	57.34%	49.97%	52.70%
		62.99%	74.74%	70.06%	69.41%	68.10%
6/23/19	Angle 3—65 cfm	56.52%	65.35%	56.17%	49.52%	59.20%
		55.71%	64.90%	56.92%	50.91%	58.70%
6/24/19	Angle 3—55 cfm	41.86%	56.33%	45.53%	33.46%	47.00%
		47.12%	61.60%	52.25%	43.38%	52.60%
6/24/19	Two vents—55 cfm ⁽²⁾	51.25%	59.07%	47.48%	38.43%	52.90%
		45.55%	57.64%	46.84%	34.99%	49.50%
6/25/19	Three vents—55 cfm	54.59%	62.95%	53.75%	47.81%	57.00%
		47.63%	56.27%	43.11%	32.73%	49.30%
6/26/19	Angle 1—55 cfm	52.23%	66.78%	59.06%	41.14%	58.20%
		51.67%	63.12%	51.28%	41.10%	54.90%
6/28/19	Angle 3—35 cfm	42.57%	49.99%	40.45%	27.70%	44.30%
		43.13%	51.10%	38.96%	28.04%	44.70%
6/28/19	Angle 3—55 cfm	52.75%	60.37%	51.53%	39.84%	54.70%
		59.73%	64.34%	52.97%	42.88%	59.70%
6/29/19	Angle 3—80 cfm	62.37%	64.96%	56.62%	43.74%	61.70%
		55.81%	63.14%	52.43%	40.54%	57.20%
6/29/19	Angle 2—55 cfm	53.14%	54.73%	43.54%	34.56%	51.40%
		50.90%	60.75%	52.83%	41.70%	54.40%
6/18/19	Angle 4—55 cfm	52.24%	57.50%	46.13%	32.94%	52.40%
		55.05%	62.01%	51.69%	39.87%	56.40%
6/30/19	Closer vent—55 cfm	58.32%	65.42%	57.04%	51.95%	60.20%
		49.57%	56.55%	46.10%	37.59%	50.90%
6/30/19	Middle vent—55 cfm	45.47%	53.20%	36.07%	20.26%	45.60%
		55.43%	62.22%	50.99%	32.57%	56.40%

⁽¹⁾ Vent Location A and C; ⁽²⁾ Vent Location B and C

One-Factor ANOVA Results

Air Flow Rates

0, 15 cfm for TTHM

<i>Source of Variation</i>	<i>SS</i>	<i>df</i>	<i>MS</i>	<i>F</i>	<i>P-value</i>	<i>F crit</i>
Between Groups	0.427787	1	0.427787	583.7579	3.3E-07	5.987378
Within Groups	0.004397	6	0.000733			
Total	0.432184	7				

15, 35 cfm for TTHM

<i>Source of Variation</i>	<i>SS</i>	<i>df</i>	<i>MS</i>	<i>F</i>	<i>P-value</i>	<i>F crit</i>
Between Groups	0.006087	1	0.006087	32.38421	0.00471	7.708647
Within Groups	0.000752	4	0.000188			
Total	0.006839	5				

0, 15 cfm for CHCl₃

<i>Source of Variation</i>	<i>SS</i>	<i>df</i>	<i>MS</i>	<i>F</i>	<i>P-value</i>	<i>F crit</i>
Between Groups	0.50717	1	0.50717	281.1044	2.87E-06	5.987378
Within Groups	0.01082	6	0.00180			
Total	0.51800	7				

0, 15 cfm for CHClBr₂

<i>Source of Variation</i>	<i>SS</i>	<i>df</i>	<i>MS</i>	<i>F</i>	<i>P-value</i>	<i>F crit</i>
Between Groups	0.218702	1	0.218702	353.6784	1.46E-06	5.987378
Within Groups	0.00371	6	0.000618			
Total	0.222412	7				

15, 35 cfm for CHClBr₂

<i>Source of Variation</i>	<i>SS</i>	<i>df</i>	<i>MS</i>	<i>F</i>	<i>P-value</i>	<i>F crit</i>
Between Groups	0.010681	1	0.010681	56.47443	0.00168	7.708647
Within Groups	0.000756	4	0.000189			
Total	0.011437	5				

35, 55 cfm for CHClBr₂

<i>Source of Variation</i>	<i>SS</i>	<i>df</i>	<i>MS</i>	<i>F</i>	<i>P-value</i>	<i>F crit</i>
Between Groups	0.015734	1	0.015734	17.46125	0.0139	7.708647
Within Groups	0.003604	4	0.000901			
Total	0.019339	5				

0, 15 cfm for CHBr₃

Source of Variation	SS	df	MS	F	P-value	F crit
Between Groups	0.128078	1	0.128078	252.5174	3.94E-06	5.987378
Within Groups	0.003043	6	0.000507			
Total	0.131121	7				

35, 55 cfm for CHBr₃

Source of Variation	SS	df	MS	F	P-value	F crit
Between Groups	0.019267	1	0.019267	12.3200	0.0247	7.708647
Within Groups	0.006255	4	0.001564			
Total	0.025522	5				

Blower angle

Angle 1, Angle 2 for CHBr₃

Source of Variation	SS	df	MS	F	P-value	F crit
Between Groups	0.005551	1	0.005551	7.696601	0.03224	5.987378
Within Groups	0.004328	6	0.000721			
Total	0.009879	7				

Number of vents

0, 1

Source of Variation	SS	df	MS	F	P-value	F crit
Between Groups	0.769293	1	0.769293	388.3977	1.11E-06	5.987378
Within Groups	0.011884	6	0.001981			
Total	0.781177	7				

0, 2

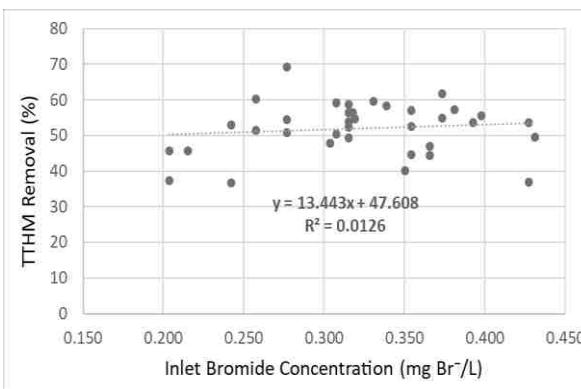
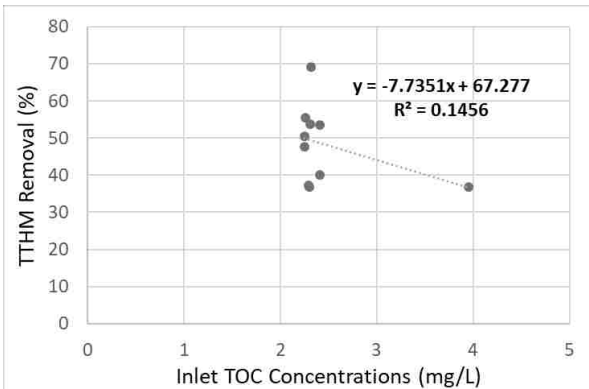
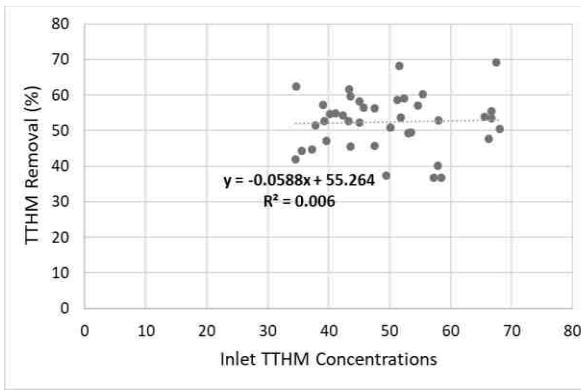
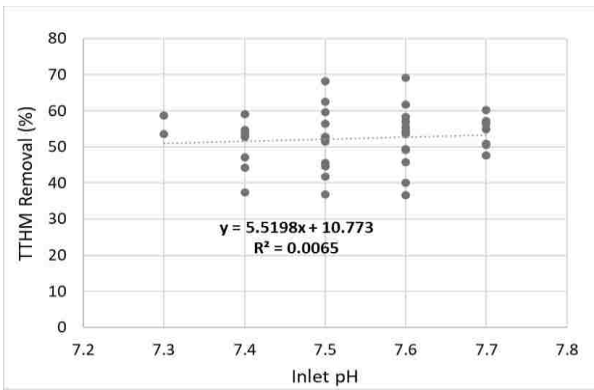
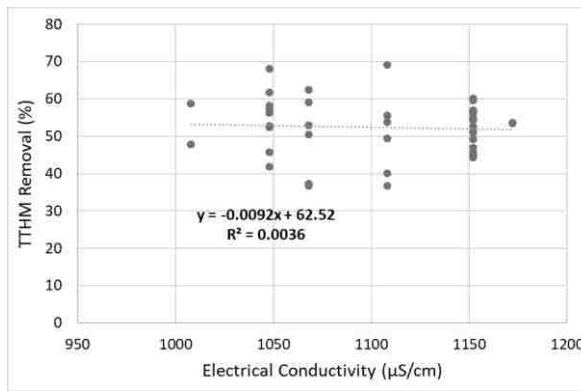
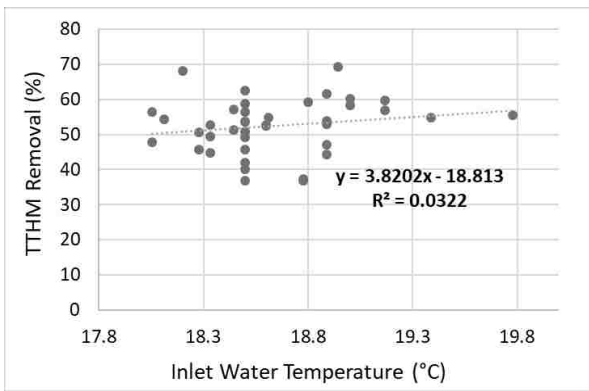
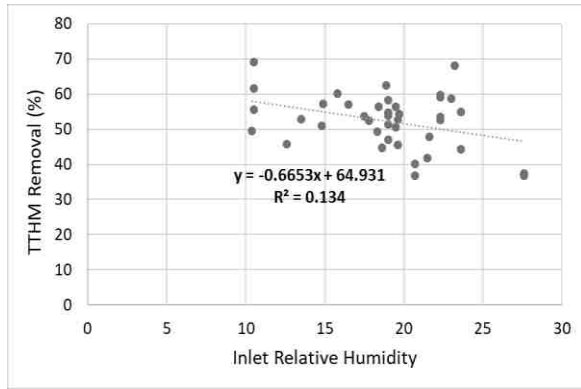
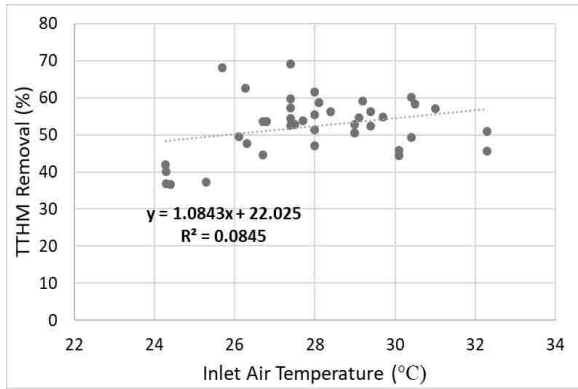
Source of Variation	SS	df	MS	F	P-value	F crit
Between Groups	0.474819	1	0.474819	448.4235	2.94E-05	7.708647
Within Groups	0.004235	4	0.001059			
Total	0.479055	5				

Vent Location

Location B, Location C

Source of Variation	SS	df	MS	F	P-value	F crit
Between Groups	0.024204162	1	0.024204162	7.002976	0.057202	7.708647
Within Groups	0.013825072	4	0.003456268			
Total	0.038029233	5				

Correlation graphs with R² values for monitored water quality results and air conditions



Appendix B

Determining the droplets flow regimes from the exit of the nozzle to the water surface at small-time intervals depends on Newton's second law, in which the sum of forces acting on a particle is equal to the mass of the particle multiplied by the acceleration. Shown below are nozzle characteristics provided by the manufacturer that were used to calculate droplets exit velocity, travel distance, travel time, and vertical and horizontal velocities.

WL4 Nozzle Characteristics			
Pressure (psi)	Orifice diameter, d_{orifice} (in)	Flow rate, Q_w (gpm)	Spray angle, (α) (deg)
20	0.188	2.90	90

T=25 °C; P=0.94 atm; MW of water (humid)=28.8 g/mol; kinematic viscosity (ν) = 1.12E-05; dynamic viscosity (μ)=1.20E-05 kg/m-s

Since the spray angle was 90° (45° from the horizontal direction and 45° vertical direction), this angle was selected to calculate for water droplets regime in the headspace.

Droplets Travel Path						
Vertical distance (cm)	$\alpha/2$ (deg)	$\alpha/2$ (rad)	$\sin(\alpha/2)$ (rad)	$\cos(\alpha/2)$ (rad)	Travel distance to water (cm)	Travel time along the path, t_{path} (s)
92	45	0.785	0.707	0.707	129	0.128

The exit velocity (v_o) is:

$$v_o = \frac{Q}{A_{\text{orifice}}} = \frac{2.89 \text{ gpm}}{\frac{\pi}{4} (0.478 \text{ cm})^2} = 10.1 \frac{\text{m}}{\text{s}}$$

Thus, both the exit (initial) velocity components in the horizontal and vertical were 7.12 m/s.

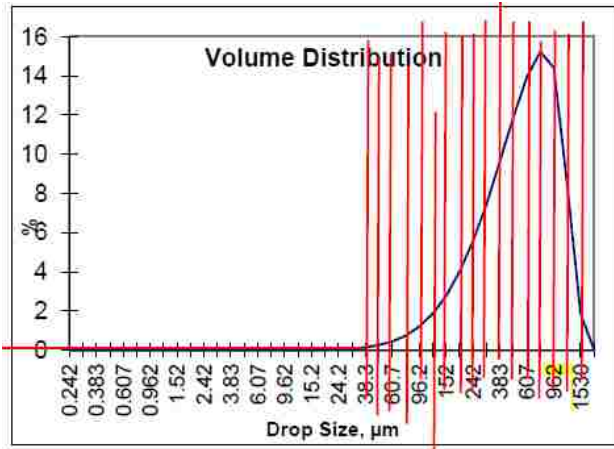
Shown below are equations for drag force acting on the droplet, terminal velocity, horizontal stop distance, and flow regime over time intervals.

Stokesian Regime	(Re<2)	$C_D = \frac{24}{Re}$	$F_d = 3\pi d_p \mu_F v$	
Horizontal	$x = -\tau * v_{0,x} \left(e^{-\left(\frac{t}{\tau}\right)} - 1 \right)$ where $\tau = \frac{\rho_p d_p^2}{18\mu_F}$		$v_x = v_{0,x} e^{-\frac{t}{\tau}}$	$x_{stop} = \tau * v_{0,x}$
Vertical	$v_y = (v_{0,y} - \tau g) e^{-\frac{t}{\tau}} + \tau g$		$v_y = (v_{0,y} - \tau g) e^{-\frac{t}{\tau}} + \tau g$	$v_t = \frac{(\rho_p - \rho_F) g d_p^2}{18\mu_F}$
	$y = -\tau(v_{0,y} - \tau g) \left(e^{-\frac{t}{\tau}} - 1 \right) + \tau g t$			
Transitional Regime	(500<Re<2)	$C_D = \frac{18.5}{Re^{0.6}}$	$F_d = 2.31\pi d_p^{1.4} \mu_F^{0.6} \rho_F^{0.4} v^{1.4}$	
Horizontal	$v_x = [v_{0,x}^{-0.4} + 0.4kt]^{-2.5}$ where $k = \frac{13.875\rho_F^{0.4}\mu_F^{0.6}}{\rho_p d_p^{1.6}}$		$x'_{stop} = \frac{1.667}{k} \left[\frac{1}{v_{0,x}^{-0.6}} - \frac{1}{1.4k(0.4kt' + v_{0,x}^{-0.4})^{1.5}} \right]$	
	$t' = \frac{1}{1.4k} \left[(v_{Re=2})^{-0.4} - \frac{1}{v_{0,x}^{0.4}} \right] = \frac{1}{1.4k} \left[\left(\frac{2\mu_F}{\rho_F d_p} \right)^{-0.4} - \frac{1}{v_{0,x}^{0.4}} \right]$			
Vertical	Change vertical velocity (v_y) with time can be found by numerically integrating: $\int_{v_{0,y}}^{v_y} \frac{dv}{g - kv^{1.4}} = \int_0^t dt$		$v_t = \frac{0.153\rho_p^{0.714} d_p^{1.14} g^{0.714}}{\rho_F^{0.286} \mu_F^{1.14}}$	
Turbulent Regime	(Re>500)	$C_D = 0.44$	$F_d = 0.055\pi d_p^2 \rho_F v^2$	
Horizontal	$v_x = \frac{1}{\left[\frac{1}{v_{0,x}} + 0.330 \left[\frac{\rho_F}{\rho_p d_p} \right] t \right]}$		$x''_{stop} = \frac{3.03\rho_p d_p}{\rho_F} \left[\ln \left(\frac{3.0303\rho_F t''}{\rho_p d_p} + \frac{1}{v_{0,x}} \right) \right]$	
	$t'' = 3.03 \left[\frac{\rho_p d_p}{\rho_F} \right] \left[\frac{1}{v_{500}} - \frac{1}{v_{0,x}} \right] = 3.03 \left[\frac{\rho_p d_p}{\rho_F} \right] \left[\frac{\rho_F d_p}{500\mu_F} - \frac{1}{v_{0,x}} \right]$			
Vertical	Change vertical velocity (v_y) with time can be found by numerically integrating: $\int_{v_{0,y}}^{v_y} \frac{dv}{g - bv^2} = \int_0^{t''} dt$		$v_t = 1.74 \left(\frac{\rho_p d_p}{\rho_F} \right)^{0.5} g^{0.5} = \sqrt{\frac{g}{b}}$ where $b = \frac{0.33*\rho_F}{d_p*\rho_p}$	
	$v_y = v_t'' * \frac{(\alpha - \exp(-2\sqrt{gb}t))}{(\exp(-2\sqrt{gb}t) + \alpha)} = \sqrt{\frac{g}{b}} * \frac{(\alpha - \exp(-2\sqrt{gb}t))}{(\exp(-2\sqrt{gb}t) + \alpha)}$ where $\alpha = \frac{1+v_{0,y}*\sqrt{\frac{b}{g}}}{1-v_{0,y}*\sqrt{\frac{b}{g}}}$			

where

- C_D =drag coefficient
- F_d = drag force acting on the droplet
- μ_F = the dynamic viscosity of the medium
- ρ_p = the particle's density
- ρ_F = the medium's density
- g is the gravitational force
- d_p = the droplet's diameter
- t = the droplet's travel time from the nozzle
- t = the droplet's travel time from the nozzle
- t = the droplet's travel time from the nozzle
- t'' = time at which the flow regime changes from turbulent to transitional
- y = vertical distance traveled
- t' = time at which the flow regime changes from transitional to Stokesian
- x = travel distance
- x_{stop} = The stop distance in the Stokesian regime
- x'_{stop} = horizontal stop distance in the transitional regime
- x''_{stop} = the horizontal stop distance in the turbulent regime
- v = the droplet's velocity
- v_x = horizontal velocity
- v_y = vertical velocity
- $v_{0,x}$ = initial horizontal velocity
- $v_{0,y}$ = initial vertical velocity
- $v_{Re=2}$ = the velocity in which Re number equals 2, or once the droplet changes from transitional to Stokesian regime
- $v_{Re=500}$ = the velocity in which the Re number equals 500, or once the droplet changes from turbulent to transitional regime
- v_t = terminal vertical velocity at infinite time

Shown below are the volume distribution and calculated fraction of volume for each droplet size.



Lower d (μm)	Upper d (μm)	Nominal drop diameter (μm)	Fraction of volume
		3.83	0.0010
3.83	6.07	4.82	0.0025
		6.07	0.0040
6.07	9.82	7.72	0.0080
		9.82	0.0150
9.82	15.2	12.22	0.0200
		15.20	0.0250
15.2	24.2	19.18	0.0400
		24.20	0.0550
24.2	38.3	30.44	0.0740
		38.30	0.0975
38.3	60.7	48.22	0.1150
		60.70	0.1400
60.7	96.2	76.42	0.1500
		96.20	0.1400
96.2	153	121.32	0.0750
		153.00	0.0150
Total			0.977

Shown below, most of the droplets exited the nozzle with transitional and turbulent regimes, and most remained in those regimes upon water surface impact.

Nominal drop diameter (μm)	Initial Re number along path	Line of flight regime	Horizontal and vertical initial Re number ⁽¹⁾	Horizontal and vertical initial regime	Vertical regime upon surface impact	Horizontal regime upon surface impact
3.83	3.44E+01	trans	2.43E+01	trans		Stokes
4.82	4.33E+01	trans	3.06E+01	trans		Stokes
6.07	5.45E+01	trans	3.86E+01	trans		Stokes
7.72	6.94E+01	trans	4.91E+01	trans		Stokes
9.82	8.82E+01	trans	6.24E+01	trans	Stokes	Stokes
12.22	1.10E+02	trans	7.76E+01	trans		trans
15.20	1.37E+02	trans	9.66E+01	trans	trans	trans
19.18	1.72E+02	trans	1.22E+02	trans		trans
24.20	2.17E+02	trans	1.54E+02	trans		trans
30.44	2.74E+02	trans	1.93E+02	trans		trans
38.30	3.44E+02	trans	2.43E+02	trans		trans
48.22	4.33E+02	trans	3.06E+02	trans		trans
60.70	5.45E+02	turb	3.86E+02	trans		trans
76.42	6.87E+02	turb	4.86E+02	trans		trans
96.20	8.64E+02	turb	6.11E+02	turb		trans
121.32	1.09E+03	turb	7.71E+02	turb		turb
153.00	1.37E+03	turb	9.72E+02	turb	turb	turb

⁽¹⁾ both initial vertical and horizontal velocities = 7.12 m/s; trans—transitional; turb—turbulent; Stokes—Stokesian;

$$\text{Individual drop volume} = \pi d^3$$

$$\text{Volumetric flow rate} = \text{Water flow rate} * \text{Fraction of volume}$$

$$\text{Number of drops per second} = \text{Individual drop volume} * \text{Individual drop volume}$$

$$\text{Drop surface area} = \pi d^2$$

$$\text{Surface area per time} = \text{Drop surface area} * \text{Number of drops per second}$$

$$\text{Surface area} = \text{Surface area per time} * t_{\text{path}}$$

Nominal drop diameter (μm)	Fraction of volume	Volumetric flow rate ⁽¹⁾ (cm ³ /sec)	Individual drop volume (cm ³ /sec)	Number of drops per second (s ⁻¹)	Drop surface area (cm ²)	Surface area per time (cm ² /s)	Surface area in the air ⁽²⁾ (cm ²)
3.83	0.001	0.18	2.94E-08	6.13E+06	4.61E-05	2.83E+02	3.62E+01
4.82	0.003	0.45	5.87E-08	7.68E+06	7.30E-05	5.61E+02	7.18E+01
6.07	0.004	0.72	1.17E-07	6.16E+06	1.16E-04	7.13E+02	9.13E+01
7.72	0.008	1.44	2.41E-07	5.99E+06	1.87E-04	1.12E+03	1.44E+02
9.82	0.015	2.71	4.96E-07	5.46E+06	3.03E-04	1.65E+03	2.12E+02
12.22	0.020	3.61	9.55E-07	3.78E+06	4.69E-04	1.77E+03	2.27E+02
15.20	0.025	4.51	1.84E-06	2.45E+06	7.26E-04	1.78E+03	2.28E+02
19.18	0.040	7.21	3.69E-06	1.95E+06	1.16E-03	2.26E+03	2.89E+02
24.20	0.055	9.92	7.42E-06	1.34E+06	1.84E-03	2.46E+03	3.15E+02
30.44	0.074	13.35	1.48E-05	9.03E+05	2.91E-03	2.63E+03	3.37E+02
38.30	0.098	17.59	2.94E-05	5.98E+05	4.61E-03	2.76E+03	3.53E+02
48.22	0.115	20.74	5.87E-05	3.53E+05	7.30E-03	2.58E+03	3.30E+02
60.70	0.140	25.25	1.17E-04	2.16E+05	1.16E-02	2.50E+03	3.19E+02
76.42	0.150	27.06	2.34E-04	1.16E+05	1.83E-02	2.12E+03	2.72E+02
96.20	0.140	25.25	4.66E-04	5.42E+04	2.91E-02	1.57E+03	2.02E+02
121.32	0.075	13.53	9.35E-04	1.45E+04	4.62E-02	6.69E+02	8.56E+01
153.00	0.015	2.71	1.88E-03	1.44E+03	7.35E-02	1.06E+02	1.36E+01
Total	0.977	176.2		4.32E+07		2.75E+04	3.52E+03

⁽¹⁾ Water flow rate = 2.90 gpm; ⁽²⁾ t_{path} or time in the air = 0.128 s

Evaporation (%) for 80 cfm, RH_{in}=10.5, RH_{out} =92.6, air temp_{in}=27.4°C, temp_{out}=21.3°C:

$$\mathcal{H}_p = \frac{\mathcal{H}}{\mathcal{H}_s} \times 100$$

$$\frac{\mathcal{H} - \mathcal{H}_s}{T - T_s} = - \frac{C_{pA} + \mathcal{H} C_{pV}}{\lambda_s}$$

where

- \dot{M}_A = mass flow rate of dry air, lb_m/min
- C_{pA} = specific heat of dry air, Btu/lb_m
- C_{pV} = specific heat of water vapor, Btu/lb_m
- λ_s = latent heat of vaporization of water (at T_s), Btu/lb_m
- \mathcal{H}_p = percentage humidity, %
- \mathcal{H}_s = saturation humidity, lb_m moisture/lb_m dry air
- \mathcal{H} = absolute humidity, lb_m water vapor/lb_m dry air

Based on the psychrometric chart, the absolute humidity = $0.0124 \frac{\text{lb H}_2\text{O}}{\text{lb of dry air}}$ and mole fraction of water vapor = 0.020.

$$\dot{m}_A = \left(\frac{28.9 \text{ lbm}}{\text{lbmole}} \right) * \frac{0.93 \text{ atm} * 80 \text{ cfm}}{\left(0.73 \frac{\text{atm-ft}^3}{\text{lbmole} \cdot \text{°R}} \right) ((460 + 80) \text{°R})} * (1 - 0.020) = 5.35 \frac{\text{lbm}}{\text{min}}$$

$$\dot{m}_W = 0.0124 \frac{\text{lb H}_2\text{O}}{\text{lb of dry air}} * 5.35 \frac{\text{lb dry air}}{\text{min}} = 0.066 \frac{\text{lbm H}_2\text{O}}{\text{min}}$$

$$\text{Flux of water} = \frac{\dot{m}_W}{\sum \text{Surface area}} = \frac{0.066 \frac{\text{lbm H}_2\text{O}}{\text{min}}}{3.52 \text{E} + 03 \text{ cm}^2} = 1.88 \text{E} - 05 \frac{\text{lbm H}_2\text{O}}{\text{min-cm}^2}$$

Volume of inflow water for 1 HRT = 330.5 gal

$$\text{Volume of evaporated water for 1 HRT} = \dot{m}_W * 1 \text{ HRT} = 0.066 \frac{\text{lbm H}_2\text{O}}{\text{min}} * 114 \text{ min} * \frac{1 \text{ gal}}{8.34 \text{ lbm}} = 0.902 \text{ gal}$$

% loss of water for 1 HRT = 1.0%

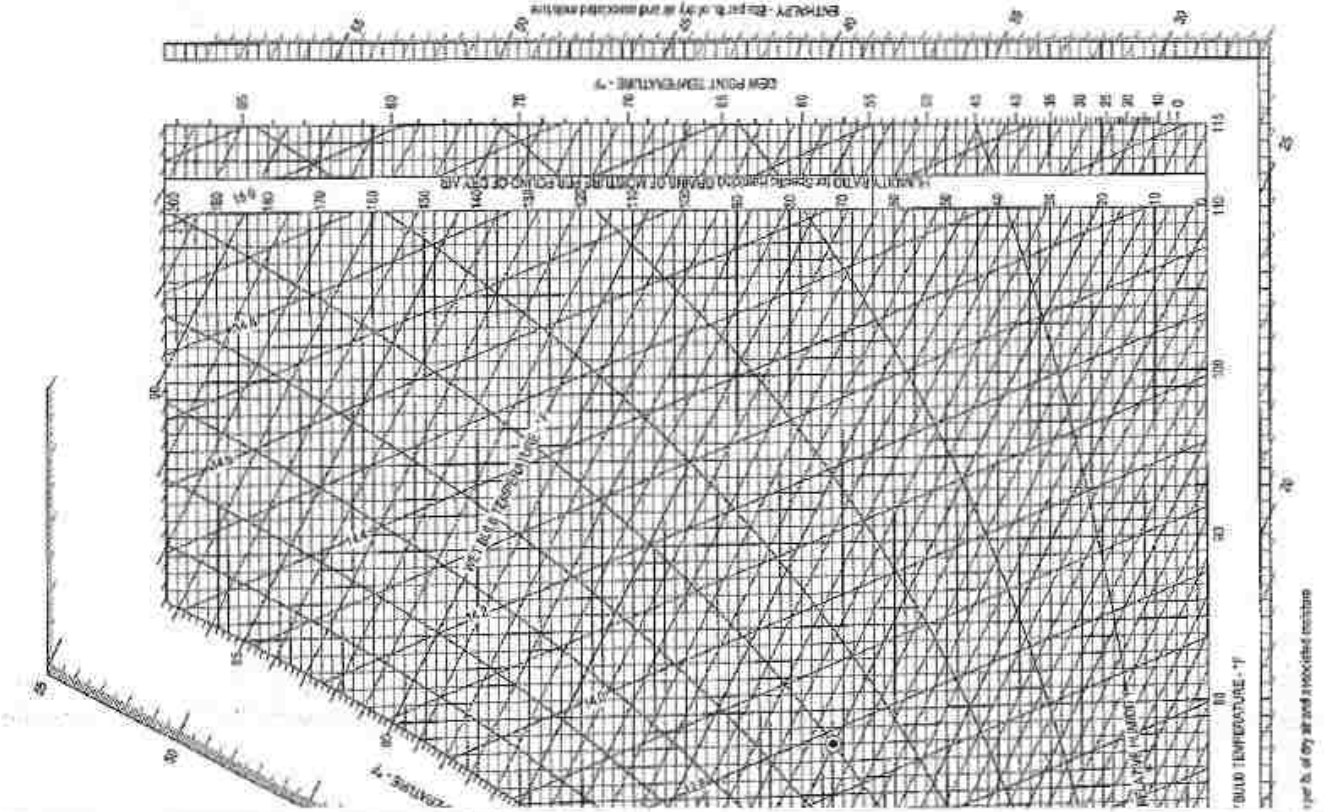
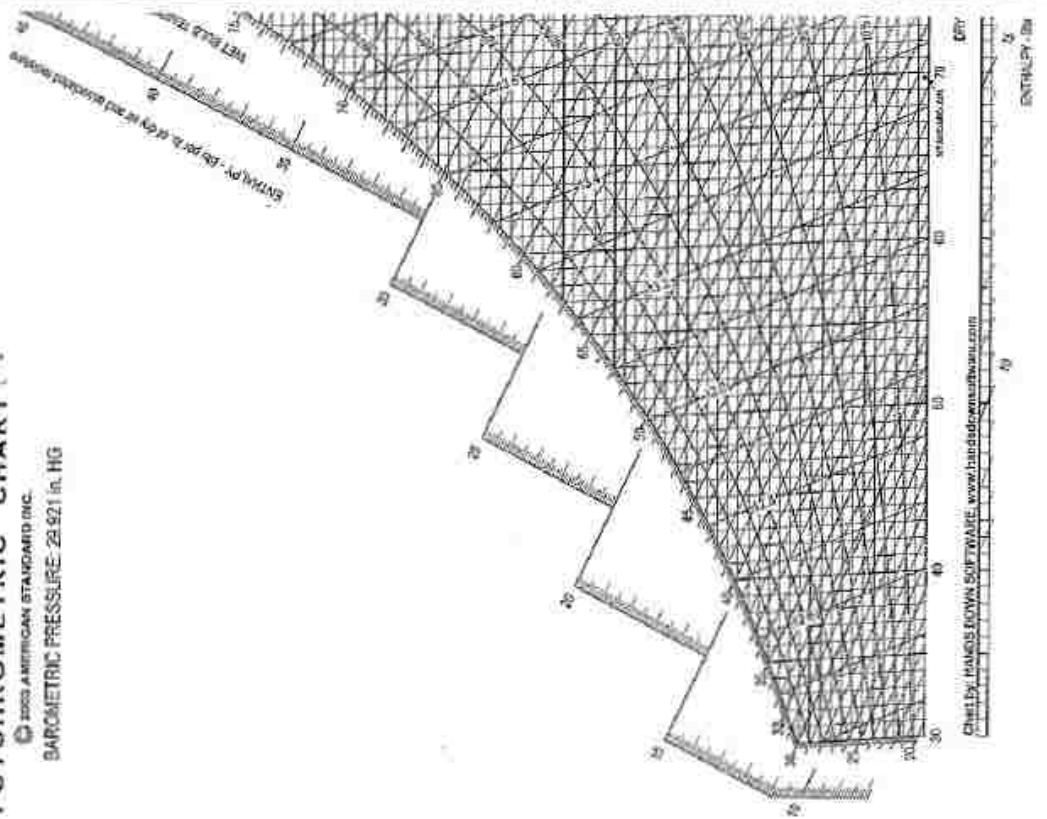
Thus, 1.0% evaporation is not substantial enough to justify the increase Br⁻ concentration.

$$\text{Final concentration of Br}^- = 101\% * 0.313 \frac{\text{mg Br}^-}{\text{L}} = 0.316 \frac{\text{mg Br}^-}{\text{L}}$$



TRANE

PSYCHROMETRIC CHART
© 2003 AMERICAN STANDARD INC.
BAROMETRIC PRESSURE: 29.921 in. HG



References

- Abdel-Wahab, A., Khodary, A., & Bensalah, N. (2010). Formation of Trihalomethanes during Seawater Chlorination. *Journal of Environmental Protection*, 01(04), 456–465.
<https://doi.org/10.4236/jep.2010.14053>
- Amy, G. L., Tan, L., & Davis, M. K. (1991). The effects of ozonation and activated carbon adsorption on trihalomethane speciation. *Water Research*, 25(2), 191–202.
[https://doi.org/10.1016/0043-1354\(91\)90029-P](https://doi.org/10.1016/0043-1354(91)90029-P)
- An, D., Gu, B., Sun, S., Zhang, H., Chen, Y., Zhu, H., ... Tong, J. (2017). Relationship between THMs/NDMA formation potential and molecular weight of organic compounds for source and treated water in Shanghai, China. *Science of the Total Environment*, 605–606, 1–8.
<https://doi.org/10.1016/j.scitotenv.2017.06.170>
- AWWA. (1997). *AWWA Standard for Welded Steel Tanks for Water Storage*. American Water Works Association.
- AWWA. (1998). Selecting and Sizing Water-Storage Tanks. *Steel Water Storage Tanks - Manual of Water Supply Practices*, (C), 53–57. Retrieved from
http://www.knovel.com.ezproxy.lib.rmit.edu.au/web/portal/browse/display?_EXT_KNOVEL_DISPLAY_bookid=3588&VerticalID=0
- Babi, K. G., Koumenides, K. M., Nikolaou, A. D., Makri, C. A., Tzoumerkas, F. K., & Lekkas, T. D. (2007). Pilot study of the removal of THMs, HAAs and DOC from drinking water by GAC adsorption. *Desalination*, 210(1–3), 215–224.
<https://doi.org/10.1016/j.desal.2006.05.046>
- Bellar, T. A., Lichtenberg, J. J., & Kroner, R. . C. (1974). The Occurrence of Organohalides in Chlorinated Drinking, 66(12), 703–706.

- Bilello, L. J., & Singley, J. E. (1986). Removing trihalomethanes by packed-column and diffused aeration. *Journal / American Water Works Association*, 78(2), 62–71.
- Bond, T., Goslan, E. H., Parsons, S. A., & Jefferson, B. (2012). A critical review of trihalomethane and haloacetic acid formation from natural organic matter surrogates. *Environmental Technology Reviews*, 1(1), 93–113.
<https://doi.org/10.1080/09593330.2012.705895>
- Brooke. (2009). Assessing Post Treatment Aeration Variables to Reduce Trihalomethanes For Small Systems.
- Brooke, E., & Collins, M. R. (2011). Posttreatment aeration to reduce THMs. *Journal - American Water Works Association*, 103(10), 84–96. <https://doi.org/10.1002/j.1551-8833.2011.tb11550.x>
- Cecchetti, A. R., Roakes, H., & Collins, M. R. (2014). Influence of selected variables on trihalomethane removals by spray aeration. *Journal - American Water Works Association*, 106(5), 91–92. <https://doi.org/10.5942/jawwa.2014.106.0021>
- Chen, H., Lin, T., Chen, W., Tao, H., & Xu, H. (2019). Removal of disinfection byproduct precursors and reduction in additive toxicity of chlorinated and chloraminated waters by ozonation and up-flow biological activated carbon process. *Chemosphere*, 216, 624–632.
<https://doi.org/10.1016/j.chemosphere.2018.10.052>
- Chowdhury, S., & Champagne, P. (2009). Risk from exposure to trihalomethanes during shower: Probabilistic assessment and control. *Science of the Total Environment*, 407(5), 1570–1578.
<https://doi.org/10.1016/j.scitotenv.2008.11.025>
- Clark, T. F. (2016). *DBP Control in an Expanding Regional Water Supply System; DBP Control in an Expanding Regional Water Supply System.*

<https://doi.org/10.5942/jawwa.2016.108.0119>

Cotruvo, J. A., & Amato, H. (2019). National Trends of Bladder Cancer and Trihalomethanes in Drinking Water: A Review and Multicountry Ecological Study. *Dose-Response*, 17(1), 155932581880778. <https://doi.org/10.1177/1559325818807781>

Duranceau, S. J., & Smith, C. T. (2016). Trihalomethane Formation Downstream of Spray Aerators Treating Disinfected Groundwater. *Journal - American Water Works Association*, 108(2), E99–E108. <https://doi.org/10.5942/jawwa.2016.108.0007>

Gerrity, D., Mayer, B., Ryu, H., Crittenden, J., & Abbaszadegan, M. (2009). A comparison of pilot-scale photocatalysis and enhanced coagulation for disinfection byproduct mitigation. *Water Research*, 43(6), 1597–1610. <https://doi.org/10.1016/j.watres.2009.01.010>

Gibert, O., Lefèvre, B., Fernández, M., Bernat, X., Paraira, M., & Pons, M. (2013). Fractionation and removal of dissolved organic carbon in a full-scale granular activated carbon filter used for drinking water production. *Water Research*, 47(8), 2821–2829. <https://doi.org/10.1016/j.watres.2013.02.028>

Krasner, S. W., Weinberg, H. S., Richardson, S. D., Pastor, S. J., Chinn, R., Scilimenti, M. J., ... Thruston, A. D. (2006). Occurrence of a new generation of disinfection byproducts. *Environmental Science and Technology*, 40(23), 7175–7185. <https://doi.org/10.1021/es060353j>

Legay, C., Rodriguez, M. J. ., B. Sérodes, J., & Levallois, P. (2010). The assessment of population exposure to chlorination by-products: A study on the influence of the water distribution system. *Environmental Health: A Global Access Science Source*, 9(1), 1–14.

Retrieved from

<http://ovidsp.ovid.com/ovidweb.cgi?T=JS&PAGE=reference&D=emed9&NEWS=N&AN=>

2010591136

- Lewis, W. K., & Whitman, W. G. (1924). Principles of Gas Absorption. *Industrial and Engineering Chemistry*, 16(12), 1215–1220. <https://doi.org/10.1021/ie50180a002>
- Li, C., Lin, Q., Dong, F., Li, Y., Luo, F., & Zhang, K. (2018). Formation of iodinated trihalomethanes during chlorination of amino acid in waters. *Chemosphere*, 217, 355–363. <https://doi.org/10.1016/j.chemosphere.2018.10.190>
- Li, X. F., & Mitch, W. A. (2018). Drinking Water Disinfection Byproducts (DBPs) and Human Health Effects: Multidisciplinary Challenges and Opportunities. *Environmental Science and Technology*, 52(4), 1681–1689. <https://doi.org/10.1021/acs.est.7b05440>
- Liu, Z., Lin, Y. L., Xu, B., Hu, C. Y., Wang, A. Q., Gao, Z. C., ... Gao, N. Y. (2018). Formation of iodinated trihalomethanes during breakpoint chlorination of iodide-containing water. *Journal of Hazardous Materials*, 353(April), 505–513. <https://doi.org/10.1016/j.jhazmat.2018.04.009>
- Marti, E. J., Pisarenko, A. N., Peller, J. R., & Dickenson, E. R. V. (2015). N-nitrosodimethylamine (NDMA) formation from the ozonation of model compounds. *Water Research*, 72. <https://doi.org/10.1016/j.watres.2014.08.047>
- Mitch, W. A., & Sedlak, D. L. (2002). Formation of N-nitrosodimethylamine (NDMA) from dimethylamine during chlorination. *Environmental Science and Technology*. <https://doi.org/10.1021/es010684q>
- Mohd Zainudin, F., Abu Hasan, H., & Sheikh Abdullah, S. R. (2018). An overview of the technology used to remove trihalomethane (THM), trihalomethane precursors, and trihalomethane formation potential (THMFP) from water and wastewater. *Journal of Industrial and Engineering Chemistry*, 57, 1–14. <https://doi.org/10.1016/j.jiec.2017.08.022>

- Munz, C., & Roberts, P. V. (1989). Gas- and liquid-phase mass transfer resistances of organic compounds during mechanical surface aeration. *Water Research*, 23(5), 589–601.
[https://doi.org/10.1016/0043-1354\(89\)90026-2](https://doi.org/10.1016/0043-1354(89)90026-2)
- Nicholson, B., Maguire, B. P., & Bursill, D. B. (1984). Henry's law constants for the trihalomethanes: effects of water composition and temperature. *Environmental Science & Technology*, 18(7), 518–521. <https://doi.org/10.1021/es00125a006>
- O'Rourke, P. J., & Amsden, A. A. (2010). The Tab Method for Numerical Calculation of Spray Droplet Breakup. *SAE Technical Paper Series*, 1. <https://doi.org/10.4271/872089>
- Padhi, R. K., Subramanian, S., & Satpathy, K. K. (2018). Formation, distribution, and speciation of DBPs (THMs, HAAs, ClO₂⁻ and ClO₃⁻) during treatment of different source water with chlorine and chlorine dioxide. *Chemosphere*, 218, 540–550.
<https://doi.org/10.1016/j.chemosphere.2018.11.100>
- Richardson, S. D. (2003). Disinfection by-products and other emerging contaminants in drinking water. *TrAC - Trends in Analytical Chemistry*, 22(10), 666–684.
[https://doi.org/10.1016/S0165-9936\(03\)01003-3](https://doi.org/10.1016/S0165-9936(03)01003-3)
- Richardson, S. D., Fasano, F., E., Ellington, J. J., Crumley, F. G., Buettner, K. M., Evans, J. J., ... Plewa, M. J. (2008). Occurrence and mammalian cell toxicity of iodinated disinfection, 42(22), 8330–8338.
- Richardson, S. D., Plewa, M. J., Wagner, E. D., Schoeny, R., & DeMarini, D. M. (2007). Occurrence, genotoxicity, and carcinogenicity of regulated and emerging disinfection by-products in drinking water: A review and roadmap for research. *Mutation Research - Reviews in Mutation Research*, 636(1–3), 178–242.
<https://doi.org/10.1016/j.mrrev.2007.09.001>

- Richardson, S. D., & Postigo, C. (2018). Liquid Chromatography–Mass Spectrometry of Emerging Disinfection By-products. *Comprehensive Analytical Chemistry*.
<https://doi.org/10.1016/bs.coac.2017.07.002>
- Roberts, P. V., & Levy, J. A. (1985). *Energy Requirements for Air Stripping Trihalomethanes. Journal (American Water Works Association) (Vol. 77)*.
- Sander, R. (2015). Compilation of Henry's law constants (version 4.0) for water as solvent. *Atmospheric Chemistry and Physics*, 15(8), 4399–4981. <https://doi.org/10.5194/acp-15-4399-2015>
- USEPA. (1996). EPA - 500 Series - 501.3 - Measurement Of Trihalomethanes In Drinking Water With Gas Chromatography/ Mass Spectrometry And Selected Ion Monitoring, 3(3), 1–19.
- USEPA. (2007). Simultaneous compliance guidance manual for the Long Term 2 and Stage 2 DBP rules. *Environmental Protection*, (March).
- USEPA. (2010). EPA 816-F-10-080 Comprehensive Disinfectants and Disinfection Byproducts Rules (Stage 1 and Stage 2): Quick Reference Guide, 4. [https://doi.org/EPA 816-F-10-080](https://doi.org/EPA%20816-F-10-080)
- USEPA. (2016). Six-Year Review 3 Technical Support Document for Disinfectants/Disinfection Byproducts Rules, 110. <https://doi.org/EPA-810-R-16-012>
- Velten, S., Knappe, D. R. U., Traber, J., Kaiser, H. P., von Gunten, U., Boller, M., & Meylan, S. (2011). Characterization of natural organic matter adsorption in granular activated carbon adsorbers. *Water Research*, 45(13), 3951–3959. <https://doi.org/10.1016/j.watres.2011.04.047>
- Volk, C., Bell, K., Ibrahim, E., Verges, D., Amy, G., & Lechevallier, M. (2000). Impact of enhanced and optimized coagulation on removal of organic matter and its biodegradable fraction in drinking water. *Water Research*, 34(12), 3247–3257.
[https://doi.org/10.1016/S0043-1354\(00\)00033-6](https://doi.org/10.1016/S0043-1354(00)00033-6)

- World Health Organization. (2011). *Guidelines for Drinking-water Quality* 4th ed., WHO, Geneva, p. 340. *World Health Organization*. [https://doi.org/10.1016/S1462-0758\(00\)00006-6](https://doi.org/10.1016/S1462-0758(00)00006-6)
- Wu, F., & Wu, S. (2009). Removal of trihalomethanes from drinking water by air stripping. *2009 International Conference on Energy and Environment Technology, ICEET 2009*, 2, 695–698. <https://doi.org/10.1109/ICEET.2009.406>
- Yang, J. S., Yuan, D. X., & Weng, T. P. (2010). Pilot study of drinking water treatment with GAC, O3/BAC and membrane processes in Kinmen Island, Taiwan. *Desalination*, 263(1–3), 271–278. <https://doi.org/10.1016/j.desal.2010.06.069>

Curriculum Vitae

The Graduate College
University of Nevada, Las Vegas

Alicia Qiu Cheung, EIT
aliciaqiu27@gmail.com

Degrees:

Bachelor of Science in Civil and Environmental Engineering, 2017

University of Nevada, Las Vegas

Master of Science in Engineering, 2019

University of Nevada, Las Vegas

Thesis Title: Impact of Ventilation on Trihalomethanes Removal by Spray Aeration

Thesis Examination Committee:

Chairperson, Dr. Erica J. Marti

Committee Member, Dr. Dave James

Committee Member, Dr. Eakalak Khan

Graduate College Representative, Dr. Jaeyun Moon